Letter (Discoveries)

Genomic signature of kin selection in an ant with obligately sterile workers

Michael R. Warner[1], Alexander S. Mikheyev[2], Timothy A. Linksvayer[1*]

[1]Department of Biology, University of Pennsylvania, Philadelphia, PA 19104, USA.

[2]Ecology and Evolution Unit, Okinawa Institute of Science and Technology, Onna-son, Okinawa, Japan 904-04012.

[*]Corresponding author. E-mail: tlinks@sas.upenn.edu

Abstract

Kin selection is thought to drive the evolution of cooperation and conflict, but the specific genes and genome-wide patterns shaped by kin selection are unknown. We identified thousands of genes associated with the sterile ant worker caste, the archetype of an altruistic phenotype shaped by kin selection, and then used population and comparative genomic approaches to study patterns of molecular evolution at these genes. Consistent with population genetic theoretical predictions, worker-upregulated genes showed relaxed adaptive evolution compared to genes upregulated in reproductive castes. Worker-upregulated genes included more taxonomically-restricted genes, indicating that the worker caste has recruited more novel genes, yet these genes also showed relaxed selection. Our study identifies a putative genomic signature of kin selection and helps to integrate emerging sociogenomic data with longstanding social evolution theory.

Kin selection theory provides the dominant framework for understanding the evolution of diverse types of social behavior, from cooperation to conflict, across the tree of life (Hamilton 1964; Bourke 2011). While kin selection theory has always had an explicit genetic focus (Hamilton 1964), researchers have made little progress in identifying specific genes that have been shaped by kin selection (Thompson et al. 2013; Ronai et al. 2016), or in identifying genome-wide evolutionary signatures of kin selection (Van Dyken and Wade 2012; Ostrowski et al. 2015). This shortfall is particularly notable in the social insects because the sterile worker caste is the archetypical example of an altruistic phenotype that evolved through kin selection (Hamilton 1964; Queller and Strassmann 1998; Bourke 2011).

The caste system of division of labor between reproductive queens and sterile workers, which first evolved in ants over 100 mya (Ward 2014), is a striking evolutionary innovation that enabled the radiation and ecological dominance of insect societies (Hölldobler and Wilson 1990). While queen and worker castes share the same genome, they express alternate suites of derived traits associated with specialization on either reproduction, or on foraging, nest defense, and brood care (Hölldobler and Wilson 1990). Because queens (and their short-lived male mates) reproduce and hence can directly pass their genes to the next generation, their traits are shaped directly by natural selection. In contrast, obligately sterile workers can only pass on their genes indirectly, by helping their fully-fertile relatives to reproduce, so that worker traits are shaped indirectly, by kin selection (Hamilton 1964; Bourke 2011). Population genetic models show that in theory, all-else-equal, genes associated with the expression of worker traits should experience relaxed rates of adaptive molecular evolution compared to genes associated with the

expression of reproductive traits, with the degree of relaxation proportional to the relatedness between workers and their fully-fertile relatives (Linksvayer and Wade 2009; Hall and Goodisman 2012; Linksvayer and Wade 2016).

Using the pharaoh ant, *Monomorium pharaonis*, a derived ant with obligately sterile workers and many queens per colony (i.e. low relatedness) (Hölldobler and Wilson 1990), in which signatures of kin selection are expected to be pronounced, we identified caste-associated genes and studied genomic signatures of short- and long-term molecular evolution of these genes. We used a large set of *M. pharaonis* samples (159 total RNA sequencing libraries; Table S1) that included a time series of developing worker and reproductive (i.e. queen and male) larvae as well as adult worker and queen head and abdominal tissue (Fig. 1A) to identify genes that were upregulated in reproductive versus worker castes. The number of differentially-expressed genes between worker and reproductive larvae at each stage increased across larval development, corresponding to divergence for overall body size (Fig. 1B; Fig. S1). Most differentially expressed genes were detected between adult queen and worker abdominal tissue (Fig. 1B), which is expected given that queens have well-developed ovaries in their abdomens while workers lack reproductive organs.

Next, to compare rates of adaptive molecular evolution at the identified worker- and reproductive-associated genes, we used a population genomic dataset based on 22 resequenced *M. pharaonis* worker genomes together with a single *M. chinense* worker genome as an outgroup. We estimated α, the proportion of amino acid substitutions fixed by positive selection (Bierne and Eyre-Walker 2004; Welch 2006; Obbard et al. 2009). This proportion for worker-associated genes (0.15, 95% CI 0.09-0.21) is approximately half that of reproductive-associated genes (0.31, 95% CI 0.26-0.38; bootstrap $p < 0.001$; Fig. 1C), indicating a relaxed rate of adaptive evolution for worker-associated genes. Estimates of mean selection coefficients and selective constraint (Fig. S3) also supported the conclusion that worker-associated genes have experienced relaxed selection compared to reproductive-associated genes. These results are consistent with theoretical expectations (Linksvayer and Wade 2009; Linksvayer and Wade 2016), providing a putative genomic signature of kin selection.

To further elucidate the evolution and genomic basis of ant caste, we used a comparative genomic approach, phylostratigraphy (Domazet-Loso et al. 2007), which estimates the evolutionary age of genes based on whether orthologs can be identified across different strata of the tree of life (i.e. phylostrata). Most of the identified worker- and reproductive-associated genes were ancient (i.e., shared across all cellular organisms, eukaryotes, or bilaterian animals; Fig. 2A), arising long before the evolution of eusociality, consistent with most non-differentially expressed genes in the *M. pharaonis* genome (Fig.

2A) as well as most genes in better annotated insect genomes (Fig. S6). Thus, the evolutionary origin and elaboration of ant caste seems to largely involve the recruitment of ancient genes, as proposed in a series of hypotheses (West-Eberhard 1996; Amdam et al. 2004; Linksvayer and Wade 2005; Amdam et al. 2006; Toth and Robinson 2007). Reproductive-associated genes, which are mainly composed of genes upregulated in adult queen tissues (Fig. S3), were especially enriched for ancient phylostrata, indicating that the evolution of the queen caste mainly involved the recruitment and long-term conservation of ancient genes involved in cellular functions (Tables S6, S7). In contrast, worker-associated genes were younger on average than reproductive-associated genes (Figs. 1D, S7)(glm, $z=10.3$, $df = 12622$, $p < 0.001$), with a relatively larger proportion of genes in younger phylostrata (Figs. 2A, S6; see also (Johnson and Tsutsui 2011; Feldmeyer et al. 2014; Harpur et al. 2014)). Interestingly, worker-associated genes in the youngest phylostrata (hymenopteran- and ant-specific genes) were enriched for chemosensory Gene Ontology categories (Table S7). These genes could putatively underlie ant-specific chemosensory adaptations, however this youngest category of worker-associated genes had α estimates that were not greater than zero (bootstrap $p = 0.86$; Fig. 2B), indicating that positive selection is not driving molecular evolution at these genes. Thus, the phylostratigraphy results provide further evidence that worker-associated genes experience relaxed selection relative to reproductive-associated genes.

Recent comparative genomic studies in bees and ants have found signatures of neutral evolution in social insect genomes, thought to be associated with reduced effective population size in species with large societies compared to solitary species (Romiguier et al. 2014; Kapheim et al. 2015). Consistent with these previous findings, our genome-wide estimate of α (0.21, 95% CI 0.17-0.27; Table S3) is lower than most previous estimates from solitary insects such as *Drosophila* (~0.5) (Bierne and Eyre-Walker 2004; Welch 2006; Obbard et al. 2009; Keightley et al. 2016). Our results indicate that the relatively low genome-wide adaptive substitution rates are at least in part a result of relaxed selection on worker-associated genes, so that neutral evolutionary processes are likely to be especially important for worker-associated genes. It is commonly assumed that intraspecific and interspecific variation for worker morphology and behavior is adaptive (Hölldobler and Wilson 1990; Ferster et al. 2006; Pie and Traniello 2007), but our results suggest that relaxed selection and nonadaptive evolutionary forces also play important roles in the evolution of worker traits, in particular for species with low nestmate relatedness (e.g., due to multiple queens or multiple mating) (Helanterä et al. 2009).

The relaxed selection we observed at worker-associated genes relative to reproductive-associated genes may also result from actual relaxed phenotypic selection on worker traits, in addition to being caused by the fact that worker-associated genes experience mainly indirect selection (Linksvayer and Wade 2009; Linksvayer and Wade 2016). For example, strong phenotypic selection on reproductive traits,

caused by intersesexual conflict, is commonly thought to drive elevated rates of adaptive molecular evolution at genes with reproductive function (e.g., seminal proteins) in solitary organisms (Pröschel et al. 2006; Ellegren and Parsch 2007). Whether this pattern could also be true for social insects, where both reproductive and non-reproductive castes are essential for colony survival and reproduction, is not clear, and more research into the relative magnitude of phenotypic selection on reproductive and worker traits is required. Interestingly, some worker-associated genes in our dataset showed evidence of positive selection (Figs. S10,S11; Table S8), and α, the estimated proportion of substitutions fixed by positive selection for worker-associated genes, was greater than zero (Fig. 1C; bootstrap $p < 0.001$) and similar to the genomic background rate for non-differentially expressed genes (Fig. 1C; bootstrap $p = 0.92$). Some worker traits may simply experience strong phenotypic selection (e.g., on the number or survival of new sibling queens), overcoming the dilution effect of kin selection (Linksvayer and Wade 2009; Linksvayer and Wade 2016). In some species, phenotypic selection may even act more strongly on worker traits, as suggested by a recent honey bee population genomic study that found evidence that a set of 90 worker-upregulated genes experienced stronger selection than 79 queen-associated genes (Harpur et al. 2014).

Our study identified thousands of genes that have putatively been shaped by kin selection, and hence reveals the promise of identifying genome-wide signatures of social evolution. Our study lends support to the notion that social traits may have distinct genetic and evolutionary features (Mikheyev and Linksvayer 2015), even though the evolution of complex social traits such as caste are mainly based on the recruitment of ancient genes. Our results thus help to tie together previous sociogenomic studies, which have been motivated by concepts from Evolutionary Developmental Biology (Toth and Robinson 2007) and have stressed the importance of either highly conserved (Toth and Robinson 2007; Woodard et al. 2011; O'Connell and Hofmann 2012; Berens et al. 2015) or novel genes (Johnson and Tsutsui 2011; Ferreira et al. 2013; Feldmeyer et al. 2014; Sumner 2014; Jasper et al. 2016) for social evolution, with population genetic models based on well-established social evolution theory (Hamilton 1964; Linksvayer and Wade 2009; Hall and Goodisman 2012; Linksvayer and Wade 2016).

METHODS

Study design and sampling procedure

In order to collect a time series of developing worker and reproductive larvae, and also adult workers and queens, we set up a sacrifice study in which 30 total replicate experimental colonies were

assigned to either a queen present or queen absent treatment and then sampled at one of five time points corresponding to larval developmental stages. Queen removal stimulates the production of new reproductives (i.e. new queens and males) (Edwards 1987; Schmidt et al. 2010) so that following queen removal, a portion of young brood (eggs and 1st instar larvae) are reared as reproductives, whereas all older brood are reared as workers. We also randomly assigned each experimental colony to one of five time points (L1-L5), corresponding to five larval developmental stages.

The timing of sampling for colonies in both treatments was based on the current age of the youngest larvae present in the queen removed treatment colonies, which corresponded to brood that were eggs at the time of queen removal. Thus, we sampled the first set of colonies assigned to stage L1 approximately five days after creation, at which point nearly all eggs in queen removed colonies had hatched into 1st instar larvae. Colonies assigned to subsequent stages (L2-L5) were sampled in intervals of 3-4 days, yielding samples of colonies with L2, L3, L4, and L5 larvae. We collected the following samples from each colony: for queen present colonies, we collected worker larvae, adult worker foragers, and adult worker nurses; for queen absent colonies, we collected both worker and reproductive larvae, adult worker foragers, and adult worker nurses observed feeding worker larvae as well as adult worker nurses observed feeding reproductive larvae.

Ten individuals of each sample type were collected and pooled into a single sample. Each individual was immediately flash-frozen in liquid nitrogen after collection. Adult worker heads and gasters (i.e. the last four abdominal segments) were collected separately and removed from the body while frozen. To collect adult queen head and gaster samples, 10 mature egg-laying queens approximately 4 months old were collected from three of the genetically homogeneous stock colonies used to create the experimental colonies and processed in the same manner as adult worker samples.

RNA sequencing and mapping

We extracted RNA using RNeasy kits in accordance with manufacturer's instructions. 25 samples were removed due to contamination or degradation, as detected by an Agilent 2100 Bioanalyzer or poor yield (<50 ng RNA). After excluding these samples, we prepared 161 cDNA sequencing libraries using poly-T capture of messenger RNA and subsequent full-length amplification, as in Aird *et al.* (2013). For quality control and to estimate the dynamic range of the sequencing experiment, we added two ERCC92 (Thermo Fisher Scientific Inc.) spike-in mixes to total RNA, with half the samples randomly receiving

one or the other mix. Sequencing of the cDNA libraries was performed on an Illumina HiSeq 2000 in SE50 mode at the Okinawa Institute of Science and Technology Sequencing Center. Reads were mapped to the assembly and NCBI version 2.0 gene models (Mikheyev and Linksvayer 2015) using RSEM (Li and Dewey 2011) to obtain expected counts and fragments per kilobase mapped (FPKM).

Differential expression analysis

We removed genes with FPKM < 1 in at least half the samples of all three tissues (head, gaster, and larvae) from further analysis. We removed two samples from further analysis due to suspected contamination (see Supplemental Table 1 for numbers of samples used for subsequent analysis). We performed differential expression analysis using edgeR (Robinson and Oshlack 2010) with a GLM-like fit to the count data (McCarthy et al. 2012). In order to identify worker-upregulated and reproductive-upregulated genes, we performed differential expression analysis separately by larval stage and adult sample type, across all larval stages, and across all larval stages and adult samples together. We performed subsequent analyses using the sets of genes that had an overall average effect of caste across all larval and adult samples. We assumed that these genes were most tightly associated with worker versus reproductive function, and hence shaped primarily by indirect (i.e. kin) selection versus direct selection.

Population genomic analysis

We constructed genomic sequencing libraries for 22 single-worker specimens of *M. pharaonis* and one outgroup worker sample of *Monomorium chinense*. We chose the ingroup samples to maximize geographic coverage and to provide a representative sample of standing genetic diversity in this species. Sequencing libraries were made using Illumina Nextera kits and sequenced on an Illumina HiSeq 2000 instrument. *M. pharaonis* reads were mapped to the reference using bowtie 2 in very sensitive local mode (Langmead and Salzberg 2012), while the *M. chinense* samples were mapped using NextGenMap (Sedlazeck et al. 2013), which offers more sensitivity for divergent sequences. Subsequently, variants were called separately using GATK, FreeBayes and Samtools (Li et al. 2009; McKenna et al. 2010; Garrison and Marth 2012). These variant call sets were converted to allelic primitives using GATK, and combined into a high credibility set using BAYSIC (Cantarel et al. 2014). We subsequently removed indels, any sites with more than two alleles, with more than 10% missing data, and any with a site quality

lower than a phred score of 40 to produce the final variant call set. The effect of each variant (synonymous vs. nonsynonymous) was determined using SnpEff (Cingolani et al. 2012). We then used the resulting table of numbers of synonymous polymorphisms (P_S) and substitutions (D_S) and nonsynonymous polymorphisms (P_N) and substitutions (D_N) for input for McDonald-Kreitman (McDonald and Kreitman 1991) test-based software for estimating population genetic parameters and inferring signatures of selection (Welch 2006; Eilertson et al. 2012).

The McDonald-Kreitman test can be extended to estimate α, the proportion of amino acid substitutions that are fixed by positive selection (Bierne and Eyre-Walker 2004)(Smith and Eyre-Walker 2002; Welch 2006), as a powerful way to study genome-wide rates of adaptive molecular evolution. We estimated α for worker-upregulated, reproductive-upregulated, and non-differentially expressed genes. We used a maximum likelihood estimator developed in the software package MKtest2.0 (Welch 2006; Obbard et al. 2009) (available at http://sitka.gen.cam.ac.uk/research/welch/GroupPage/Software.html, last accessed 1 July, 2016).

Comparative genomic phylostratigraphy analysis

We constructed phylostratigraphic maps for *M. pharaonis*, as well as two species with higher quality genomes (*Apis mellifera*, and *Drosophila melanogaster*), following previously developed methods (Domazet-Loso et al. 2007; Domazet-Lošo and Tautz 2010; Quint et al. 2012; Drost et al. 2015). Phylostrata were defined for each species according to the NCBI taxonomy database (Table S4; Fig. S6). We constructed a target database by adding recently sequenced hymenopteran genomes to a database that was recently used in a phylostratigraphy study of animal and plant development (Drost et al. 2015). Species-specific amino acid sequences were downloaded from RefSeq (Pruitt et al. 2012), last accessed 11 July, 2016. Each amino acid sequence at least 30 amino acids long for each of the three species were used as a query against the target database using BLASTp (version 2.2.25). Transcripts were assigned to the oldest phylostrata containing at least one BLAST hit with an E-value below 10^{-5} for the given transcript. If no BLAST hit with an E-value below 10^{-5} was found, the transcript was placed in the youngest, species-specific phylostrata (e.g., *Monomorium pharaonis*). Genes were assigned to phylostrata based on the phylostrata of their longest transcript isoform. To verify that our results did not depend on the E-value threshold we used, we also constructed a map for *M. pharaonis* using a very liberal E-value threshold of 10^{-1} as well as the default, much more conservative 10^{-5} threshold (Quint et al. 2012).

To compare mean phylostrata between queen- and worker-associated genes, we used generalized linear models with poisson residuals (or quasipoisson for overdispersed models). We used both raw phylostrata (after removing any phylostrata with zero genes; PS in Table S4), as well as phylostrata condensed into 6 main categories because many categories had few genes (Fig. S6): cellular organisms, eukaryotes, bilaterian animals, insects, hymenopterans, and ants ("Condensed PS1" Table S4). To compare the relative contribution of phylostrata to worker- and reproductive-associated genes, we constructed contingency tables, used omnibus Chi-square tests, calculated standardized Pearson's residuals to explore the contribution of each cell to the omnibus test, and presented the results using mosaic plots with the "vcd" R package (Friendly and Meyer 2015) and the 6 Condensed PS1 categories. The significance of enrichment for individual cells was assessed with standardized Pearson residuals, where residuals with an absolute value > 2 have an approximate p-value < 0.05, and residuals with an absolute value > 4 have an approximate p-value < 0.001 (Friendly 1994)(Friendly and Meyer 2015).

Gene Ontology enrichment analysis

We calculated GO term enrichment of categories of identified worker-associated and reproductive-associated genes, as well as worker-associated and reproductive-associated genes grouped by phylostrata, using the R package "GOstats", with a cut-off p-value of 0.05 (Falcon and Gentleman 2007).

Statistical analyses

All statistical analyses and figures were made with R version 3.1.2.

Data deposition

Raw sequencing reads will be deposited in DDBJ bioproject PRJDB3164. Count and FPKM data, and a .csv file summarizing all analyses for each locus are available as Supplementary Materials.

SUPPLEMENTARY MATERIAL

Supplemental Methods, Supplemental Tables S1-S8, Supplemental Figures S1-S10, and auxiliary Supplemental Tables 1-5

ACKNOWLEDGEMENTS

This work was supported be supported by the National Science Foundation (grant number IOS-1452520 to T.A.L.) and Okinawa Institute for Science and Technology subsidy funding to A.S.M..

REFERENCES

Aird SD, Watanabe Y, Villar-Briones A, Roy MC, Terada K, Mikheyev AS. 2013. Quantitative high-throughput profiling of snake venom gland transcriptomes and proteomes (*Ovophis okinavensis* and *Protobothrops flavoviridis*). BMC Genomics 14:790.

Amdam GV, Csondes A, Fondrk MK, Page RE Jr. 2006. Complex social behaviour derived from maternal reproductive traits. Nature 439:76–78.

Amdam GV, Norberg K, Fondrk MK, Page RE Jr. 2004. Reproductive ground plan may mediate colony-level selection effects on individual foraging behavior in honey bees. Proc. Natl. Acad. Sci. U. S. A. 101:11350–11355.

Berens AJ, Hunt JH, Toth AL. 2015. Comparative transcriptomics of convergent evolution: different genes but conserved pathways underlie caste phenotypes across lineages of eusocial insects. Mol. Biol. Evol. 32:690–703.

Bierne N, Eyre-Walker A. 2004. The genomic rate of adaptive amino acid substitution in Drosophila. Mol. Biol. Evol. 21:1350–1360.

Bourke AFG. 2011. Principles of Social Evolution.

Cantarel BL, Weaver D, McNeill N, Zhang J, Mackey AJ, Reese J. 2014. BAYSIC: a Bayesian method for combining sets of genome variants with improved specificity and sensitivity. BMC Bioinformatics 15:104.

Cingolani P, Platts A, Wang LL, Coon M, Nguyen T, Wang L, Land SJ, Lu X, Ruden DM. 2012. A program for annotating and predicting the effects of single nucleotide polymorphisms, SnpEff: SNPs in the genome of Drosophila melanogaster strain w1118; iso-2; iso-3. Fly 6:80–92.

Domazet-Loso T, Brajković J, Tautz D. 2007. A phylostratigraphy approach to uncover the genomic history of major adaptations in metazoan lineages. Trends Genet. 23:533–539.

Domazet-Lošo T, Tautz D. 2010. A phylogenetically based transcriptome age index mirrors ontogenetic divergence patterns. Nature 468:815–818.

Drost H-G, Gabel A, Grosse I, Quint M. 2015. Evidence for active maintenance of phylotranscriptomic hourglass patterns in animal and plant embryogenesis. Mol. Biol. Evol. 32:1221–1231.

Edwards JP. 1987. Caste regulation in the pharaoh's ant Monomorium pharaonis: the influence of queens on the production of new sexual forms. Physiol. Entomol. 12:31–39.

Eilertson KE, Booth JG, Bustamante CD. 2012. SnIPRE: selection inference using a Poisson random effects model. PLoS Comput. Biol. 8:e1002806.

Ellegren H, Parsch J. 2007. The evolution of sex-biased genes and sex-biased gene expression. Nat. Rev. Genet. 8:689–698.

Falcon S, Gentleman R. 2007. Using GOstats to test gene lists for GO term association. Bioinformatics 23:257–258.

Feldmeyer B, Elsner D, Foitzik S. 2014. Gene expression patterns associated with caste and reproductive status in ants: worker-specific genes are more derived than queen-specific ones. Mol. Ecol. 23:151–161.

Ferreira PG, Patalano S, Chauhan R, Ffrench-Constant R, Gabaldón T, Guigó R, Sumner S. 2013. Transcriptome analyses of primitively eusocial wasps reveal novel insights into the evolution of sociality and the origin of alternative phenotypes. Genome Biol. 14:R20.

Ferster B, Pie MR, Traniello JFA. 2006. Morphometric variation in North AmericanPogonomyrmexandSolenopsisants: caste evolution through ecological release or dietary change? Ethol. Ecol. Evol. 18:19–32.

Friendly M. 1994. Mosaic Displays for Multi-Way Contingency Tables. J. Am. Stat. Assoc. 89:190.

Friendly M, Meyer D. 2015. Discrete Data Analysis with R: Visualization and Modeling Techniques for Categorical and Count Data. CRC Press

Garrison E, Marth G. 2012. FreeBayes. arXiv preprint1207.3907 [q-bio.GN] [Internet]. Available from: http://arxiv.org/abs/1207.3907

Hall DW, Goodisman MAD. 2012. The effects of kin selection on rates of molecular evolution in social insects. Evolution 66:2080–2093.

Hamilton WD. 1964. The genetical evolution of social behaviour. I. J. Theor. Biol. 7:1–16.

Harpur BA, Kent CF, Molodtsova D, Lebon JMD, Alqarni AS, Owayss AA, Zayed A. 2014. Population genomics of the honey bee reveals strong signatures of positive selection on worker traits. Proc. Natl. Acad. Sci. U. S. A. 111:2614–2619.

Helanterä H, Strassmann JE, Carrillo J, Queller DC. 2009. Unicolonial ants: where do they come from, what are they and where are they going? Trends Ecol. Evol. 24:341–349.

Hölldobler B, Wilson EO. 1990. The Ants. Harvard University Press

Jasper WC, Linksvayer TA, Atallah J, Friedman D, Chiu JC, Johnson BR. 2016. Large-Scale Coding Sequence Change Underlies the Evolution of Postdevelopmental Novelty in Honey Bees. Mol. Biol. Evol. 33:1379.

Johnson BR, Tsutsui ND. 2011. Taxonomically restricted genes are associated with the evolution of sociality in the honey bee. BMC Genomics 12:164.

Kapheim KM, Pan H, Li C, Salzberg SL, Puiu D, Magoc T, Robertson HM, Hudson ME, Venkat A, Fischman BJ, et al. 2015. Social evolution. Genomic signatures of evolutionary transitions from solitary to group living. Science 348:1139–1143.

Keightley PD, Campos JL, Booker TR, Charlesworth B. 2016. Inferring the Frequency Spectrum of Derived Variants to Quantify Adaptive Molecular Evolution in Protein-Coding Genes of Drosophila melanogaster. Genetics 203:975–984.

Langmead B, Salzberg SL. 2012. Fast gapped-read alignment with Bowtie 2. Nat. Methods 9:357–359.

Li B, Dewey CN. 2011. RSEM: accurate transcript quantification from RNA-Seq data with or without a reference genome. BMC Bioinformatics 12:323.

Li H, Handsaker B, Wysoker A, Fennell T, Ruan J, Homer N, Marth G, Abecasis G, Durbin R, 1000 Genome Project Data Processing Subgroup. 2009. The Sequence Alignment/Map format and SAMtools. Bioinformatics 25:2078–2079.

Linksvayer TA, Wade MJ. 2005. The evolutionary origin and elaboration of sociality in the aculeate Hymenoptera: maternal effects, sib-social effects, and heterochrony. Q. Rev. Biol. 80:317–336.

Linksvayer TA, Wade MJ. 2009. Genes with social effects are expected to harbor more sequence variation within and between species. Evolution 63:1685–1696.

Linksvayer TA, Wade MJ. 2016. Theoretical Predictions for Sociogenomic Data: The Effects of Kin Selection and Sex-Limited Expression on the Evolution of Social Insect Genomes. Frontiers in Ecology and Evolution [Internet] 4. Available from: http://dx.doi.org/10.3389/fevo.2016.00065

McCarthy DJ, Chen Y, Smyth GK. 2012. Differential expression analysis of multifactor RNA-Seq experiments with respect to biological variation. Nucleic Acids Res. 40:4288–4297.

McDonald JH, Kreitman M. 1991. Adaptive protein evolution at the Adh locus in Drosophila. Nature 351:652–654.

McKenna A, Hanna M, Banks E, Sivachenko A, Cibulskis K, Kernytsky A, Garimella K, Altshuler D, Gabriel S, Daly M, et al. 2010. The Genome Analysis Toolkit: a MapReduce framework for analyzing next-generation DNA sequencing data. Genome Res. 20:1297–1303.

Mikheyev AS, Linksvayer TA. 2015. Genes associated with ant social behavior show distinct transcriptional and evolutionary patterns. Elife 4:e04775.

Obbard DJ, Welch JJ, Kim K-W, Jiggins FM. 2009. Quantifying adaptive evolution in the Drosophila

immune system. PLoS Genet. 5:e1000698.

O'Connell LA, Hofmann HA. 2012. Evolution of a vertebrate social decision-making network. Science 336:1154–1157.

Ostrowski EA, Shen Y, Tian X, Sucgang R, Jiang H, Qu J, Katoh-Kurasawa M, Brock DA, Dinh C, Lara-Garduno F, et al. 2015. Genomic signatures of cooperation and conflict in the social amoeba. Curr. Biol. 25:1661–1665.

Pie MR, Traniello JFA. 2007. Morphological evolution in a hyperdiverse clade: the ant genus Pheidole. J. Zool. 271:99–109.

Pröschel M, Zhang Z, Parsch J. 2006. Widespread adaptive evolution of Drosophila genes with sex-biased expression. Genetics 174:893–900.

Pruitt KD, Tatusova T, Brown GR, Maglott DR. 2012. NCBI Reference Sequences (RefSeq): current status, new features and genome annotation policy. Nucleic Acids Res. 40:D130–D135.

Queller DC, Strassmann JE. 1998. Kin Selection and Social Insects. Bioscience 48:165–175.

Quint M, Drost H-G, Gabel A, Ullrich KK, Bönn M, Grosse I. 2012. A transcriptomic hourglass in plant embryogenesis. Nature 490:98–101.

Robinson MD, Oshlack A. 2010. A scaling normalization method for differential expression analysis of RNA-seq data. Genome Biol. 11:R25.

Romiguier J, Lourenco J, Gayral P, Faivre N, Weinert LA, Ravel S, Ballenghien M, Cahais V, Bernard A, Loire E, et al. 2014. Population genomics of eusocial insects: the costs of a vertebrate-like effective population size. J. Evol. Biol. 27:593–603.

Ronai I, Oldroyd BP, Barton DA, Cabanes G, Lim J, Vergoz V. 2016. Anarchy Is a Molecular Signature of Worker Sterility in the Honey Bee. Mol. Biol. Evol. 33:134–142.

Schmidt AM, Linksvayer TA, Boomsma JJ, Pedersen JS. 2010. Queen–worker caste ratio depends on colony size in the pharaoh ant (Monomorium pharaonis. Insectes Soc. 58:139–144.

Sedlazeck FJ, Rescheneder P, von Haeseler A. 2013. NextGenMap: fast and accurate read mapping in

highly polymorphic genomes. Bioinformatics 29:2790–2791.

Smith NGC, Eyre-Walker A. 2002. Adaptive protein evolution in Drosophila. Nature 415:1022–1024.

Sumner S. 2014. The importance of genomic novelty in social evolution. Mol. Ecol. 23:26–28.

Thompson GJ, Hurd PL, Crespi BJ. 2013. Genes underlying altruism. Biol. Lett. 9:20130395.

Toth AL, Robinson GE. 2007. Evo-devo and the evolution of social behavior. Trends Genet. 23:334–341.

Van Dyken JD, Wade MJ. 2012. Detecting the molecular signature of social conflict: theory and a test with bacterial quorum sensing genes. Am. Nat. 179:436–450.

Ward PS. 2014. The Phylogeny and Evolution of Ants. Annu. Rev. Ecol. Evol. Syst. 45:23–43.

Welch JJ. 2006. Estimating the genomewide rate of adaptive protein evolution in Drosophila. Genetics 173:821–837.

West-Eberhard MJ. 1996. Wasp societies as microcosms for the study of development and evolution. In: Turillazzi S, West-Eberhard MJ, editors. Natural history and evolution of paper wasps. New York: Oxford University Press. p. 290–317.

Woodard SH, Fischman BJ, Venkat A, Hudson ME, Varala K, Cameron SA, Clark AG, Robinson GE. 2011. Genes involved in convergent evolution of eusociality in bees. Proc. Natl. Acad. Sci. U. S. A. 108:7472–7477.

Fig. 1. Genomic signature of kin selection. (A) In order to identify genes upregulated in reproductives versus worker castes, which should be shaped mainly by direct versus indirect (i.e. kin) selection, respectively, we collected a time series of worker- and reproductive (i.e. queen and male) larvae (L2-L5), as well as adult worker and queen head and abdomen tissue samples. **(B)** Dozens to thousands of genes were differentially expressed and upregulated in either reproductive (orange) or worker (blue) castes for each larval stage and adult tissue sample. "Overall" shows genes that were differentially expressed across all samples (i.e. genes with a main effect of caste on expression). The L2 comparison is excluded from subsequent analyses because only 59 total genes were differentially expressed at this early stage. **(C)** Reproductive-upregulated genes had higher α, the proportion of amino acid substitutions fixed by positive selection, for all comparisons except for L3. NDE, non-differentially expressed genes. **(D)** Reproductive-upregulated genes were also older on average (i.e. lower mean phylostrata) for all comparisons except L3. The phylostrata were grouped into the six categories as shown in Fig. 2A, but using all original 19 categories produced the same result (Fig. S7). *** $p<0.001$.

Fig. 2. The contribution of ancient and young genes to caste evolution. (A) Most caste-associated genes, as well as NDE genes in the *M. pharaonis genome*, are from ancient phylostrata (Fig. S6). **(B)** Genes in the youngest phylostrata tend to show relaxed adaptive evolution (i.e. 95% CI of α overlapping zero), except for reproductive-associated genes in the hymenopteran & ant phylostratum. Genes in the two oldest phylostrata mainly drive the pattern of higher rates of adaptive evolution for reproductive-associated genes relative to worker-associated genes (Fig. 1C); * $p<0.05$, *** $p<0.001$. Note that negative α values are caused by sampling error or the presence of mildly deleterious mutations that segregate but do not fix (Obbard et al. 2009). The last two phylostrata (hymenopteran and ant) were combined because there are not enough ant-specific genes for accurate α estimates. **(C)** Mosaic plot showing that relative to reproductive-associated genes, worker-associated genes are enriched for the four youngest phylostrata, while reproductive-upregulated genes are enriched for the eukaryote phylostratum. The area of each cell is proportional to the number of genes in each caste and phylostrata category. Blue shading indicates overrepresentation (light blue $p < 0.05$, dark blue $p < 0.001$), and red-shading indicates underrepresentation (light red $p < 0.05$, dark red, $p < 0.001$), based on cell standardized pearson residuals.

Figure 1

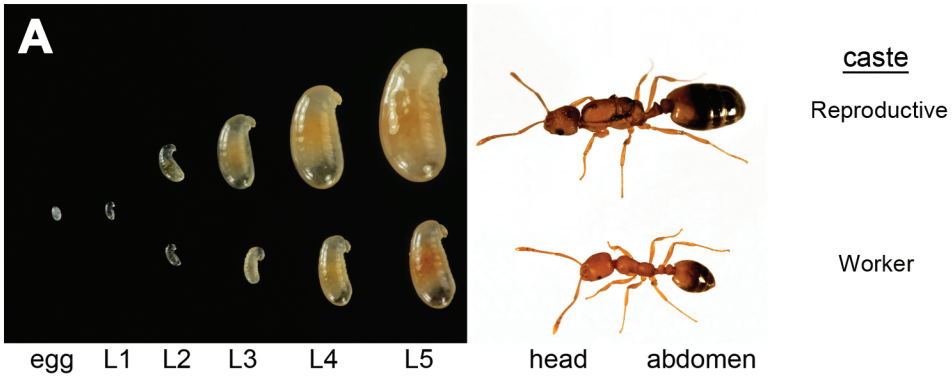

Figure 2

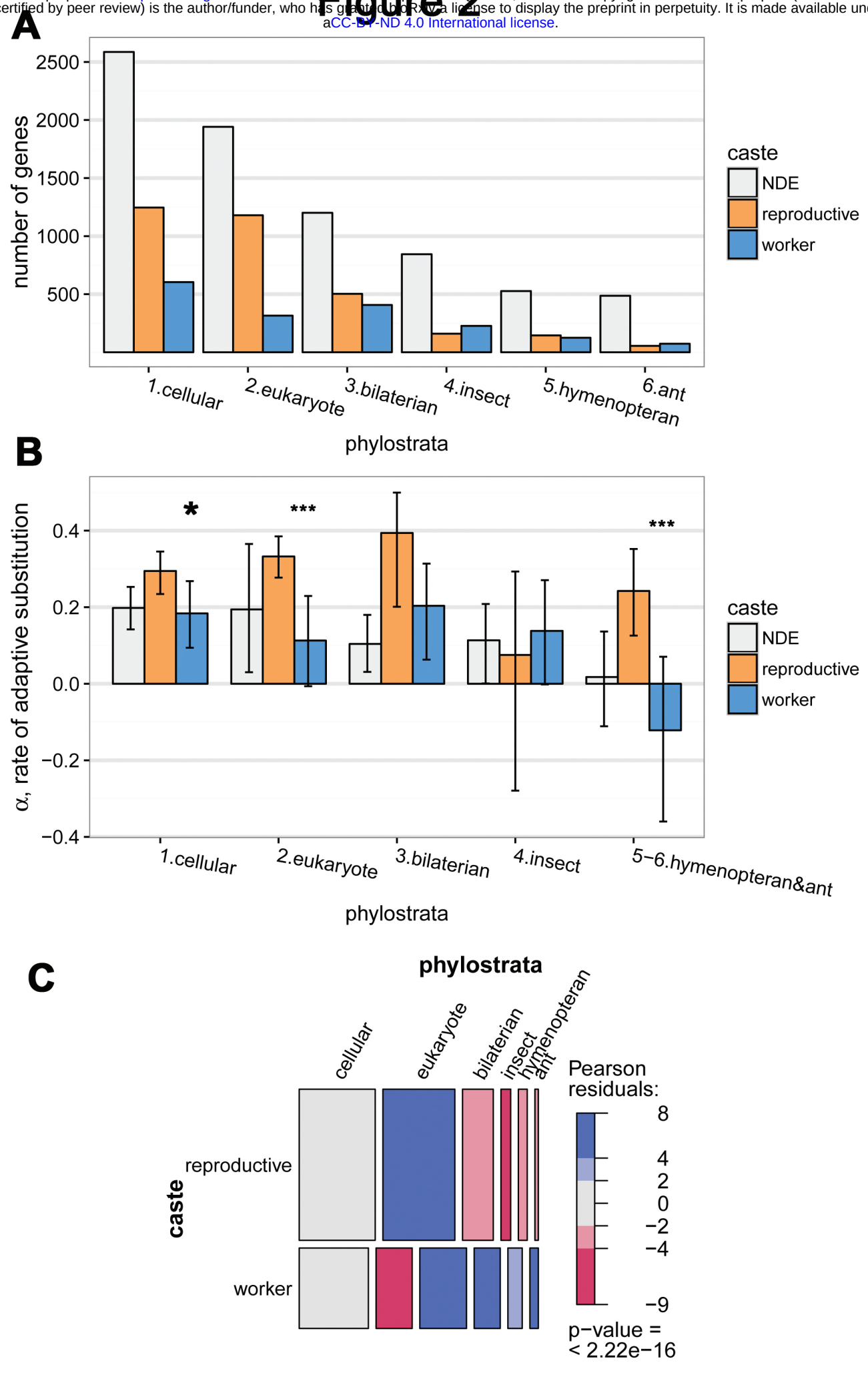

Supplementary Material

Supplemental Methods

Study species

Monomorium pharaonis has the following suite of traits that make it suitable for the current study: unlike most ants and other hymenopteran social insects, which have facultatively sterile workers that can lay male-destined eggs under some conditions, *Monomorium* workers are obligately sterile (Hölldobler and Wilson 1990), so that genes exclusively expressed by *M. pharaonis* workers can only have indirect fitness effects; *M. pharaonis* colonies are readily experimentally induced to shift from producing only new workers, to producing a mixture of new workers and reproductives (i.e. queens and males), by removing current egg-laying queens (Schmidt et al. 2010)(Edwards 1987); worker- and reproductive-destined larvae can be morphologically distinguished at an early developmental stage (Fig. 1A) (Berndt and Kremer 1986a); controlled crosses can readily be made in the lab and hundreds of colonies kept across generations; and aggression between workers from different colonies is transient so that the genetic makeup of colonies can be experimentally controlled.

Study design and colony setup

The study was run in three total blocks, each separated by three weeks, starting in April 2014. For each block, we did the following:

1. We created a genetically homogeneous source by mixing at least 10 large stock colonies, which themselves had been repeatedly mixed across generations (note that unlike most ants, *M. pharaonis* colonies display at most transient aggression following colony mixing).
2. From this source, we allocated 0.5 mL of mixed brood and workers to each replicate experimental colony, resulting in colonies with ~300-400 workers and ~300-400 brood of various stages (i.e. eggs, larvae, pupae).
3. We randomly assigned half of the experimental colonies to a queen present treatment, where queen number was standardized to 10 queens, and the other half to a queen absent treatment, where all queens were removed. Queen removal stimulates the production of new reproductives (i.e. new queens and males) (Schmidt et al. 2010)(Edwards 1987) so that following queen removal, a portion of young brood (eggs and 1st instar larvae) are reared as reproductives, whereas all older brood are reared as workers.
4. We also randomly assigned each experimental colony to one of five time points (L1-L5), corresponding to five larval developmental stages (see below).

All colonies were maintained at 27 ± 1 ºC and 50% humidity, and fed twice weekly with dried mealworms (*Tenebrio molitor*) and an agar-based synthetic diet (Dussutour and Simpson 2008). Experimental colonies were maintained in glass nests made of two pieces of 4 cm x 6 cm glass separated by 1.5 mm strips of plastic. All surveys and sampling were performed using dissecting microscopes.

Sampling procedure

Note that adult *M. pharaonis* workers performing foraging or nursing tasks have been

shown to have divergent whole-body gene expression profiles (Mikheyev and Linksvayer 2015), and we collected forager and nurse samples across social contexts (queen presence and larval stage) in order to be able to confidently identify genes that are upregulated in worker tissues.

On the day designated for sample collection, colonies were placed in petri dishes, surveyed, and then lightly anesthetized using carbon dioxide to prepare the colony for sample collection. While anesthetized, the top glass pane of the nest was removed to enable collection of nursing workers, the petri dish was covered with a lid to minimize disturbance from air flow, and the petri dish was placed on a heating pad, kept at 27 ºC, to maintain a constant temperature throughout sample collection. Colonies were left undisturbed for 30 minutes to recover from anesthesia prior to sample collection. Foragers were collected when observed collecting food outside the nest, and nurses were collected when observed nursing the appropriate larval stage. For example, for the L2 sample, worker nurses were collected when witnessed feeding a 2nd instar worker larva, and reproductive nurses when witnessed feeding a 2nd instar reproductive larva. After all foragers and nurses were collected, colonies were lightly anesthetized again and larvae of the appropriate stage were collected.

Larval instars were determined by overall size, shape, and especially hair presence and morphology (Berndt and Kremer 1986b). *M. pharaonis* larvae have three distinct larval instars (Berndt and Kremer 1986b), but because the vast majority of growth occurs in the third larval instar, we divided the third instar into three separate stages (L3-L5) based on size (Fig. 1A). Third instar worker larvae were defined as the L3 stage until they reached 0.75x the length of a worker pupa, L4 stage up to 1x the length of worker pupae, and L5 thereafter. Reproductive larvae are hairless (Berndt and Kremer 1986b) and can be differentiated from worker larvae starting at the 2nd larval instar. Reproductive larval stages were defined as follows: 2nd instar (i.e. L2) until 0.5x the length of a worker pupa, L3 from 0.5-1x the length of a worker pupae, L4 from 1-1.5x the length of a worker pupa, and L5 thereafter.

Note that it is not possible to morphologically distinguish between male and queen larvae, so that the reproductive larvae we collected included both males and queens. *M. pharaonis* colonies produce female-biased reproductive sex ratios (e.g., 0.739 female [queen/(queen+male)], interquartile range = 0.028, based on 39 colonies, (Schmidt et al. 2010)), and furthermore, newly eclosed adult queens are on average 1.42 times as large as males (1.359 mg wet mass versus 0.955 mg, based on samples of 247 newly eclosed queens and 235 males, (Schmidt et al. 2010)). Thus, we estimate that approximately 80% of the sampled larval tissue came from queens, so that the transcriptomic profiles we observed for our reproductive larvae samples mostly reflected queen larvae.

We separately collected adult head and abdominal tissues to increase the likelihood of detecting differentially expressed genes associated with adult behavior (e.g., genes upregulated in worker brains) and function (e.g., genes upregulated in queen reproductive tissues).

Differential expression analysis

For stage-specific analyses, caste was the only factor included. For analyses including all larval samples or all adult and larval samples, we used a model with caste and stage as fixed factors. For comparisons only considering larval stages, we included batch as an additional factor, but

we could not include batch in comparisons including adult samples because the queen samples were not collected within the same blocked design.

Population genomic analyses

The McDonald-Kreitman test (McDonald and Kreitman 1991) uses both polymorphism and substitution data (e.g., an excess of nonsynonymous substitutions relative to polymorphisms; $D_N/D_S > P_N/P_S$) to infer the fixation of advantageous mutations by positive selection (Bierne and Eyre-Walker 2004). This approach is more powerful at identifying signatures of positive selection than using only substitution data for divergent lineages (i.e. with d_N/d_S, which is D_N/D_S weighted by the total numbers of nonsynoymous and synonymous sites), because elevated d_N/d_S estimates can arise either from positive selection or relaxed purifying selection.

MKtest2.0 was especially suitable for our needs because it can simultaneously estimate α for different gene categories (Obbard et al. 2009), instead of only providing a single genome-wide estimate. Besides estimating α, MKtest2.0 can estimate other population genetic parameters, including selective constraint, described by 1-*f*, the proportion of non-synonymous mutations that experience strong purifying selection, as well as neutral diversity, and neutral divergence. Because we were interested in comparing patterns of selection experienced by worker- and reproductive-upregulated genes, and to avoid overparameterized models, we focused on α and *f* and kept other parameters at default values (i.e. a single global value). We compared model estimates for α and *f* and model fit statistics using a single genome-wide estimate (i.e. the default), separate estimates for each of three categories (i.e. reproductive-associated, worker-associated, and NDE), and for *f*, we also considered separate estimates for each locus. Because models with gene-specific *f* estimates were best (Table S6), we focus on the estimates from these models in the main text, although we observed similar patterns for other parameters as well. We estimated 95% confidence intervals for α with the bootstrapping feature in MKtest2.0 (i.e. as 95% bootstrap intervals around the mean, based on 1,000 bootstrap replicates across genes). We also used bootstrapping to determine p-values for the hypothesis that reproductive-associated genes have α greater than worker-associated genes. Similarly, we used bootstrapping to determine p-values for the hypothesis that caste-associated genes grouped by phylostrata had α greater than zero. We used beta regression (R package "betareg"; (Cribari-Neto and Zeileis 2010)), to compare mean *f* estimates between worker-associated and queen-associate genes.

In addition to estimating α across groups of genes in order to compare rates of adaptive molecular evolution at these genes, it is possible to estimate selection coefficients separately for each locus and then compare mean estimated selection coefficients. The software SnIPRE (Eilertson et al. 2012), Selection Inference using Poisson Random Effects, is a Bayesian implementation of the McDonald-Kreitman test and seeks to estimate several population genetic parameters similar to those estimated by MKtest2.0, including the selection coefficient acting on every gene weighted by effective population size ($\gamma = 2N_e s$). We used SnIPRE to estimate γ for each gene and compared mean γ for the categories of caste-associated genes we identified. Specifically, we used a generalized linear model (glm) to compare mean BSnIPRE.est, a normalized estimate of γ produced by SnIPRE, for worker-associated, reproductive-associated, and NDE genes.

We also used SnIPRE to categorize genes as experiencing positive, neutral, or negative selection. We also classified genes as experiencing selection using the standard McDonald-Kreitman test (McDonald and Kreitman 1991), by plotting log(p-value) from this test versus the -log(*NI*) (Li et al. 2008), where NI is the neutrality index. We used an unbiased estimator for NI (Stoletzki and Eyre-Walker 2010). Genes above a threshold p-value from the McDonald-Kreitman test with a positive -log(*NI*) were categorized as having experienced positive selection, and those with a negative -log(*NI*) were categorized as having experienced negative selection (Li et al. 2008). We used both a liberal cutoff of 0.05 for the nominal p-value from the McDonald-Kreitman test, and also a much more conservative Bonferroni-corrected p-value cutoff (Li et al. 2008) based on the 5,674 genes included in the analysis (genes with zeros for any of the four counts D_N,D_S, P_N,P_S were excluded because such zeros lead to undefined *NI*).

Comparative genomic phylostratigraphy analysis

Phylostratigraphy attempts to estimate the evolutionary age of protein-coding genes in a focal species by identifying the distribution of their homologs across the tree of life (Domazet-Loso et al. 2007; Domazet-Lošo and Tautz 2010; Quint et al. 2012; Drost et al. 2015). The approach sorts genes into hierarchical phylostrata (PS), based on the oldest BLAST hit of their amino acid sequence. For example, a gene from an ant species with identified orthologs across all eukaryotes is assumed to be much older than a gene with only identifiable orthologs in other closely related ant species. We were interested in estimating the relative ages of the the sets of worker-upregulated, reproductive-upregulated, and non-differentially expressed genes that we identified, and were less interested in the precise age estimates. Indeed, even though phylostratigraphy has been widely used (Domazet-Loso et al. 2007; Domazet-Lošo and Tautz 2010; Quint et al. 2012; Drost et al. 2015), the precise age estimates can be influenced by several factors, including parameters used to define homology in BLAST (e.g., threshold gene length, threshold E-value, database size, etc.) (Moyers and Zhang 2016)(Moyers and Zhang 2015). Furthermore, because homologous sequences in BLAST are generally required to span relatively small lengths (i.e. 30 amino acids) (Quint et al. 2012; Drost et al. 2015), small portions of a gene can impact the phylostrata assigned.

Statistical analyses and figures

All statistical analyses and figures were made with R version 3.1.2, using packages “ggplot2”, ”gplots”, ”scales”, “stats”, “plyr”, “ggdendro”, “gridExtra”, “tidyr”, ”plyr”, ”vcd”, ”vcdExtra”, “Vennerable”, ”data.table”, “edgeR”, “myTAI”, “betareg”, and “GOstats”. Complete R scripts used in the analyses will be included in the final publication. For Figure 1A, we collected representative worker and reproductive larvae from each stage (Berndt and Kremer 1986b) and arranged them in a series in order to produce a figure representing the developmental time series we used.

Figures and Tables

Fig. S1. Log2 fold change (Reproductive/Worker) as a function of the mean of worker and reproductive expression (FPKM) across all larval stages and adult samples. Genes with

annotation information and FPKM > 500 and a LogFC of a greater magnitude than 2.5 are labeled. Genes that are colored are differentially expressed, with a main effect of caste across samples: orange = reproductive-upregulated; blue = worker-upregulated; grey = non-differentially expressed (NDE). For plotting purposes, genes with a log2 fold greater than (less than) 5 (-5) assigned a value of 5 (-5). Genes with greater mean expression than 1000 FPKM assigned a value of 1000 FPKM.

Fig S2. Log2 fold change (Reproductive/Worker) as a function of the mean of worker and reproductive expression (FPKM) for specific larval stages or adult samples. Results are from (**A**) across larval stages L2-L5, (**B**) adult head, (**C**) adult gaster, (**D**) L2, (**E**) L3, (**F**) L4, and (**G**) L5. Genes that are colored are differentially expressed, with a main effect of caste across samples: orange = reproductive-upregulated; blue = worker-upregulated; grey = NDE. For plotting purposes, genes with a log2 fold greater than (less than) 5 (-5) were assigned a value of 5 (-5). Genes with greater mean expression than 1000 FPKM were assigned a value of 1000 FPKM.

Fig. S3. Weighted three-set Venn diagrams showing the contribution of: **A.** queen gaster-upregulated genes, queen head-upregulated genes, and the union of all reproductive larvae-upregulated genes (for L2-L5) to the set of reproductive-upregulated genes with a main effect across all samples; **B.** Worker gaster-upregulated genes, worker head-upregulated genes, and the union of all worker larvae-upregulated genes (for L2-L5) to the set of worker-upregulated genes with a main effect across all samples. Note that the set of reproductive-upregulated genes is dominated by genes upregulated in adult queen tissues, with 80% of reproductive-upregulated genes upregulated in queen abdominal (i.e. gaster) tissue, and 46% in queen head tissue. 41% (i.e. 1341/3252) are only upregulated in queen gasters, and not in any other tissue. In contrast, the set of worker-upregulated genes is more evenly composed of genes upregulated in worker gaster, head, and larval samples.

Fig. S4. Per-locus selective constraint and selection coefficients across samples. (**A**) Reproductive-upregulated genes with a main effect across all samples ("overall") and reproductive-upregulated genes from queen abdomens had higher mean selective constraint (=lower *f*) than worker-upregulated genes. Locus-specific *f* estimates were made with MKtest2.0. (**B**). Except for the L3 comparison, reproductive-upregulated genes in all comparisons have higher mean selection coefficients estimated by SnIPRE (glm using the normalized estimate BSnIPRE.est). For L3, worker-associated genes have a higher estimate than reproductive associated genes. * $p < 0.05$, ** $p < 0.01$, *** $p < 0.001$.

Fig. S5. (**A**) Number of differentially expressed genes for only larval samples (L3-L5) as well as "overall larvae", genes with a main effect of caste across larval samples. (**B**) Reproductive-associated genes have higher α, the proportion of amino acid substitutions fixed by positive selection, for larval genes, except at the L3 stage. * $p < 0.05$, ** $p < 0.01$.

Fig. S6. Number of genes in each phylostrata, as defined by the NCBI taxonomy database for: (**A**) *M. pharaonis* (E-value = 1×10^{-5}), (**B**) *M. pharaonis* (E-value = 1×10^{-1}), (**C**) *D. melanogaster* (E-value = 1×10^{-5}), (**D**) *A. mellifera* (E-value = 1×10^{-5}). The overall distribution is similar for all

three species, with the majority of genes being ancient, and the pattern observed for *M. pharaonis* is consistent even when a very liberal threshold (E-value = 1 x 10^{-1}) is used. BLASTp hits are made against a database containing nearly all species with curated genome annotations, with a minimum match length of 30 amino acids and a maximum E-value as listed above.

Fig. S7. Using the original 19 phylostrata, reproductive-upregulated genes were older on average (i.e. lower mean phylostrata) for all comparisons except L3, the same result as when using grouped phylostrata (Fig. 1D). *** p<0.001.

Fig. S8. Mosaic plot showing the relative contribution of phylostrata to sets of reproductive-associated, worker-associated, and NDE genes. As when only considering worker- and reproductive-associated genes (Fig. 2C), reproductive-associated genes are enriched for the eukaryote phylostratum, but also for the cellular organism phylostratum. Similarly, worker-associated genes are enriched for bilaterian animal and insect phylostrata, but relative to NDE genes are no longer significantly enriched for the youngest two phylostrata (hymenopteran and ant) (Fig. 2C). The area of each cell is proportional to the number of genes in each caste and phylostrata category. Blue shading indicates overrepresentation (light blue $p < 0.05$, dark blue $p < 0.001$), and red-shading indicates underrepresentation (light red $p < 0.05$, dark red, $p < 0.001$), based on cell standardized pearson residuals.

Fig. S9. P-value as calculated from the McDonald-Kreitman test plotted against the neutrality index, which has been -log transformed, such that positive values indicate positive selection and negative indicate purifying/balancing selection. The solid black line indicates the nominal p-value (0.05) while the dashed line indicates the p-value after Bonferroni correction (N = 5674). Genes are colored by differential expression: grey = non-differentially expressed; orange = reproductive; blue = worker. For plotting purposes, genes with p-values less than 1 x 10^{-10} were assigned a p-value of 1 x 10^{-10}, and those with a -log transformed neutrality index of greater (less) than 3 (-3) were assigned a value of 3 (-3).

Fig. S10. Overlap of A) positively and B) negatively selected genes as defined by SNiPRE and the Neutrality Index. Genes with negative values of -log10(Neutrality Index) and p-values less than 0.05 (for nominal) are defined by the "NI" method as under purifying selection, while such genes with positive -log10(Neutrality Index) values are assigned to the positive selection category. "NI, B-F correction" uses the same method but the p-value cutoff from the MKtest is adjusted for multiple comparisons using the Bonferroni procedure.

Figure S1

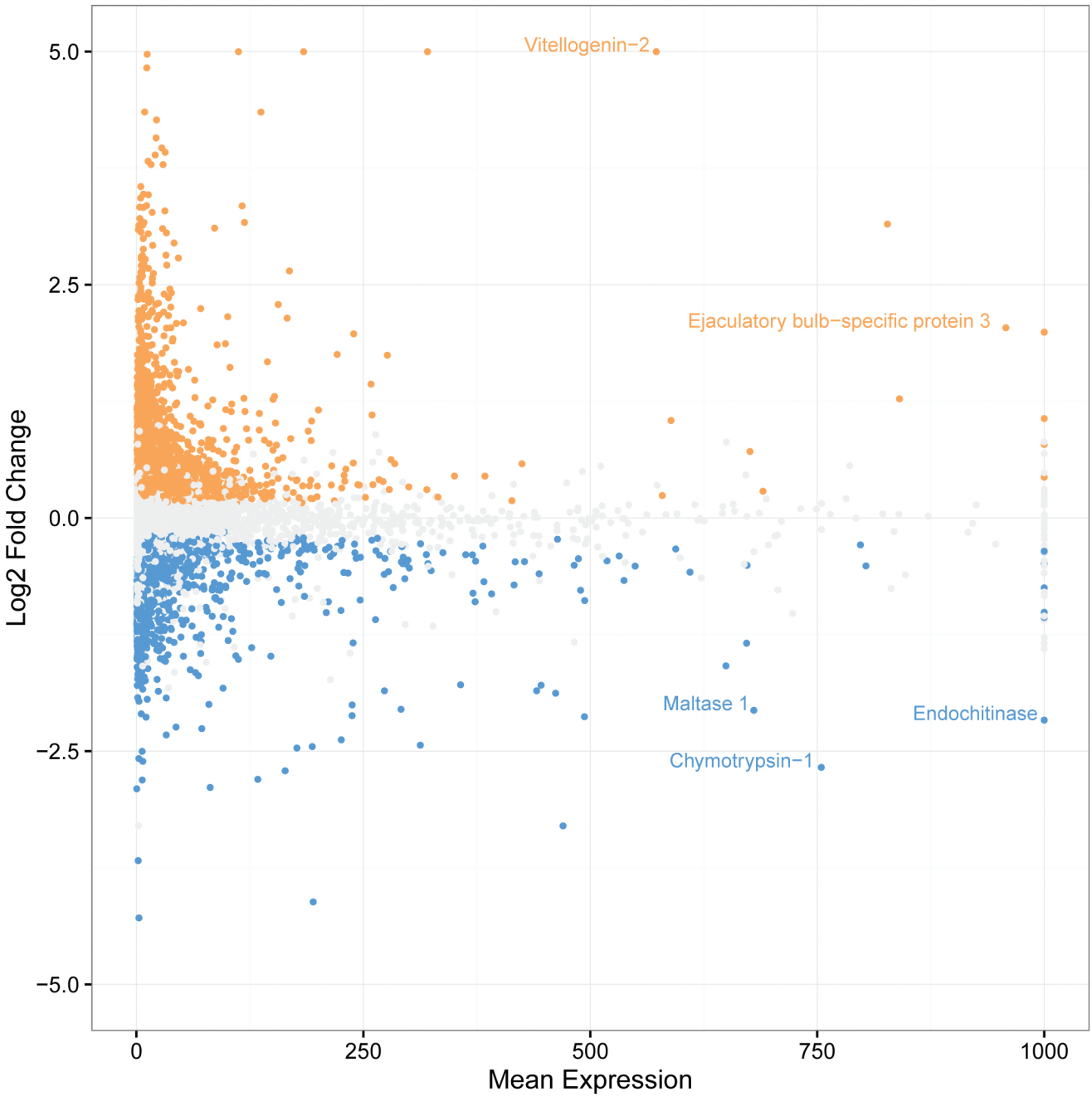

Figure S2

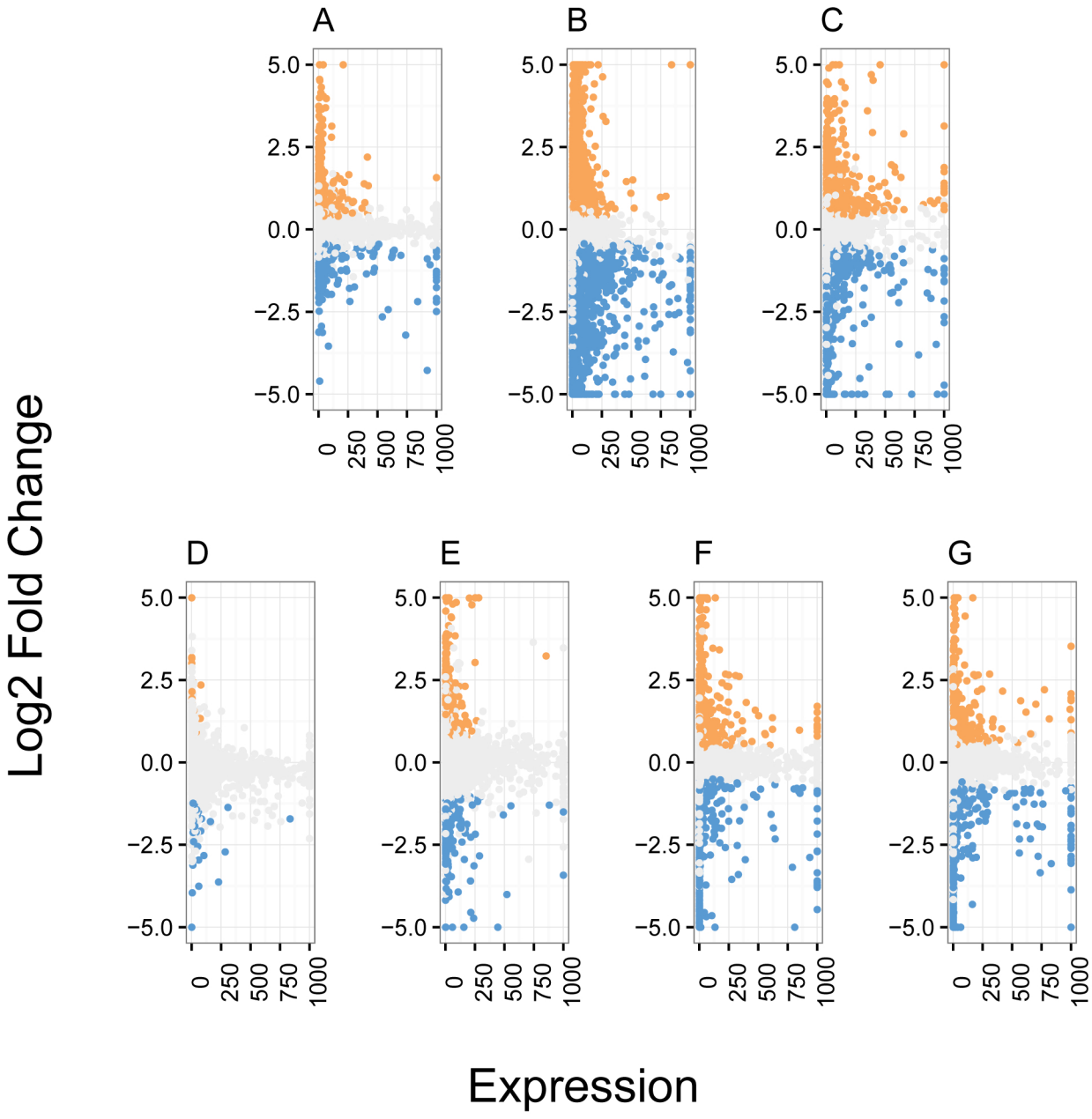

Figure S3

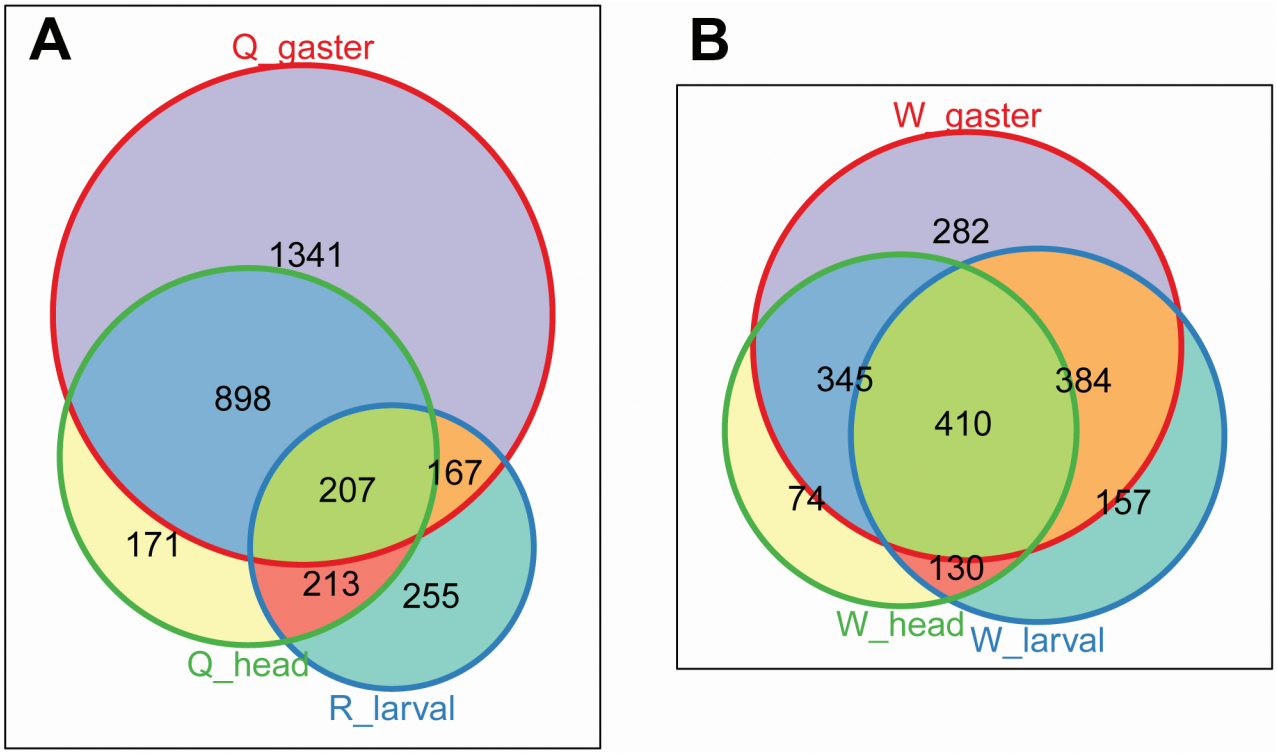

Figure S4

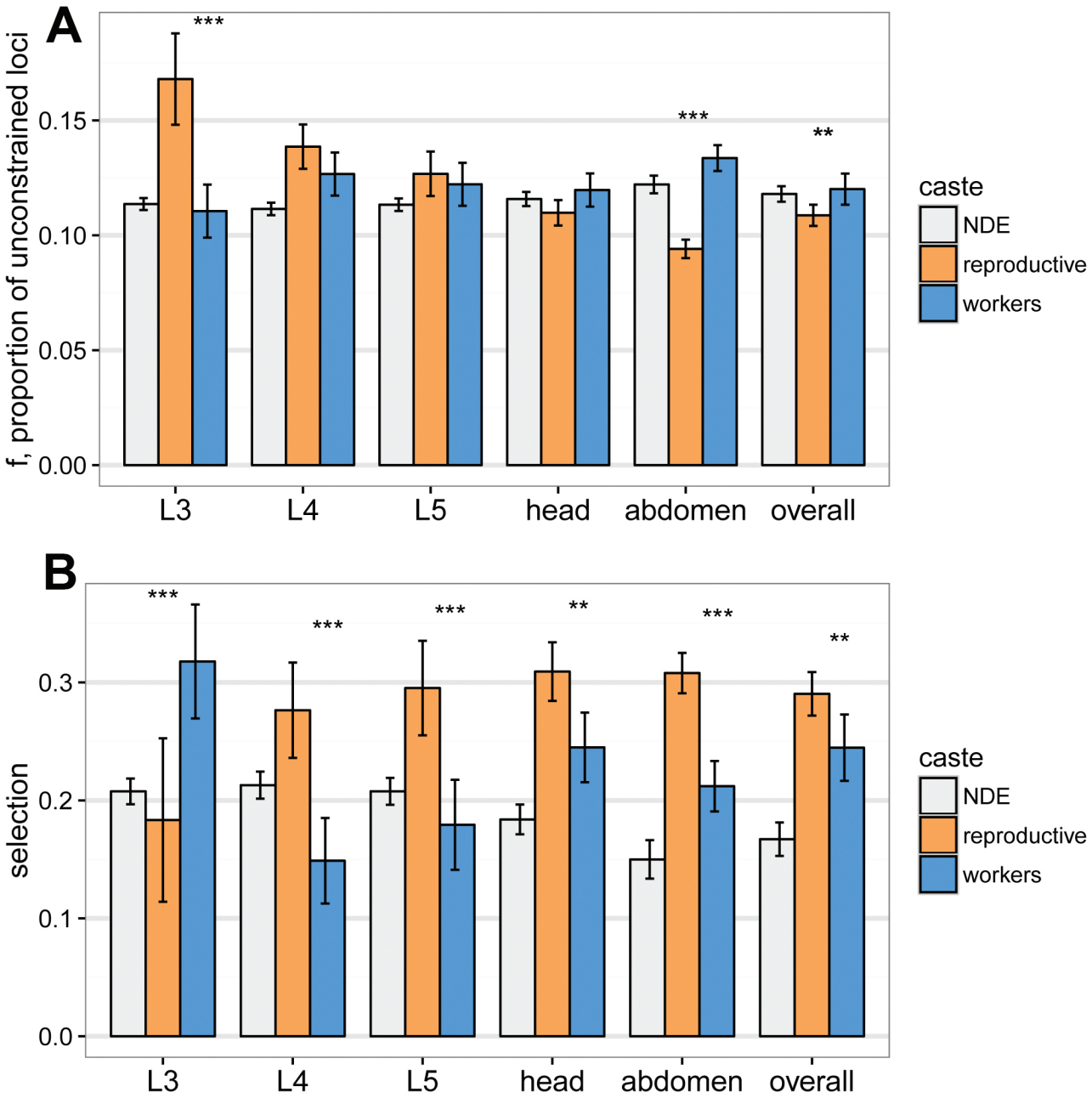

Figure S5

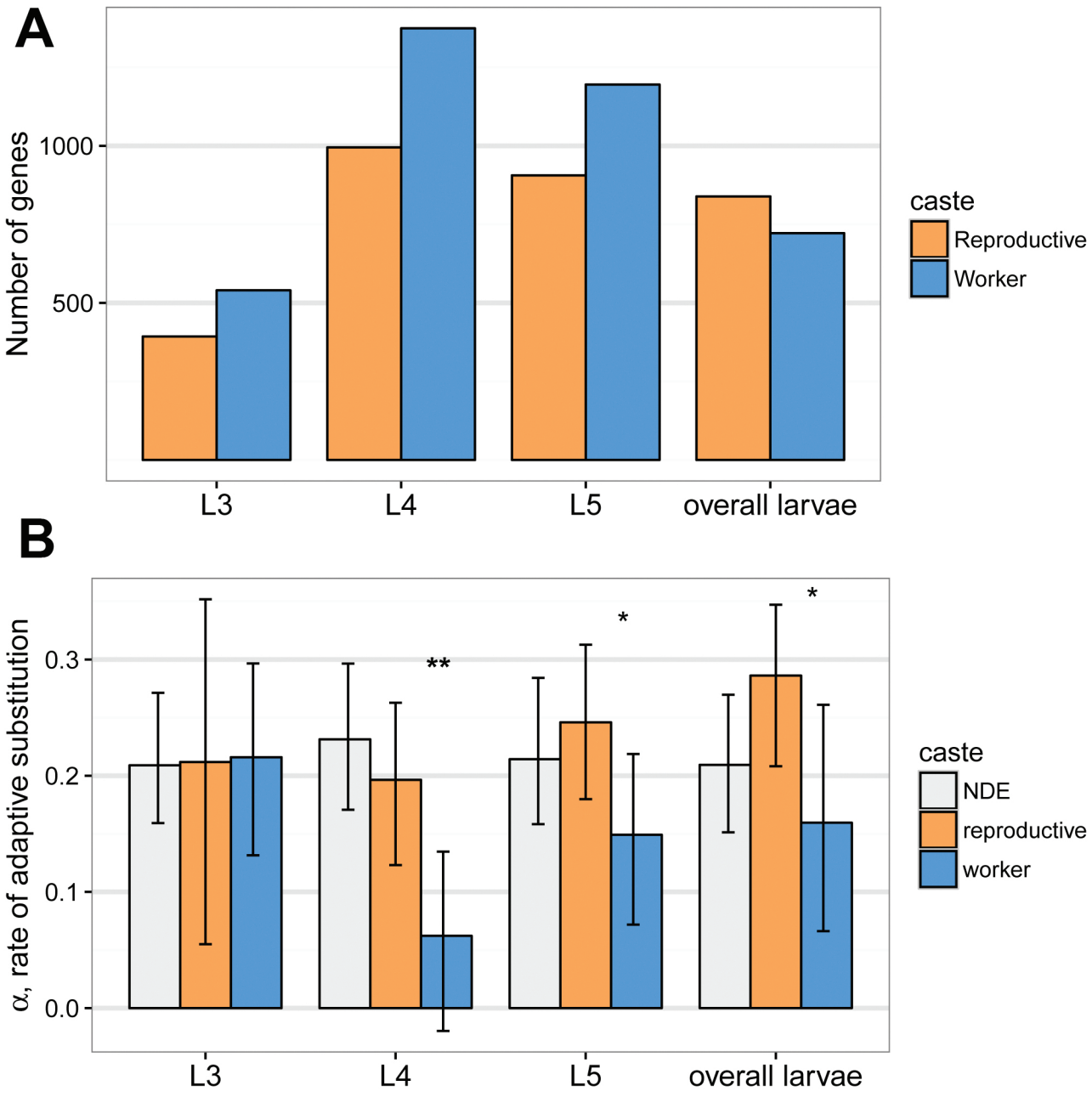

Figure S6

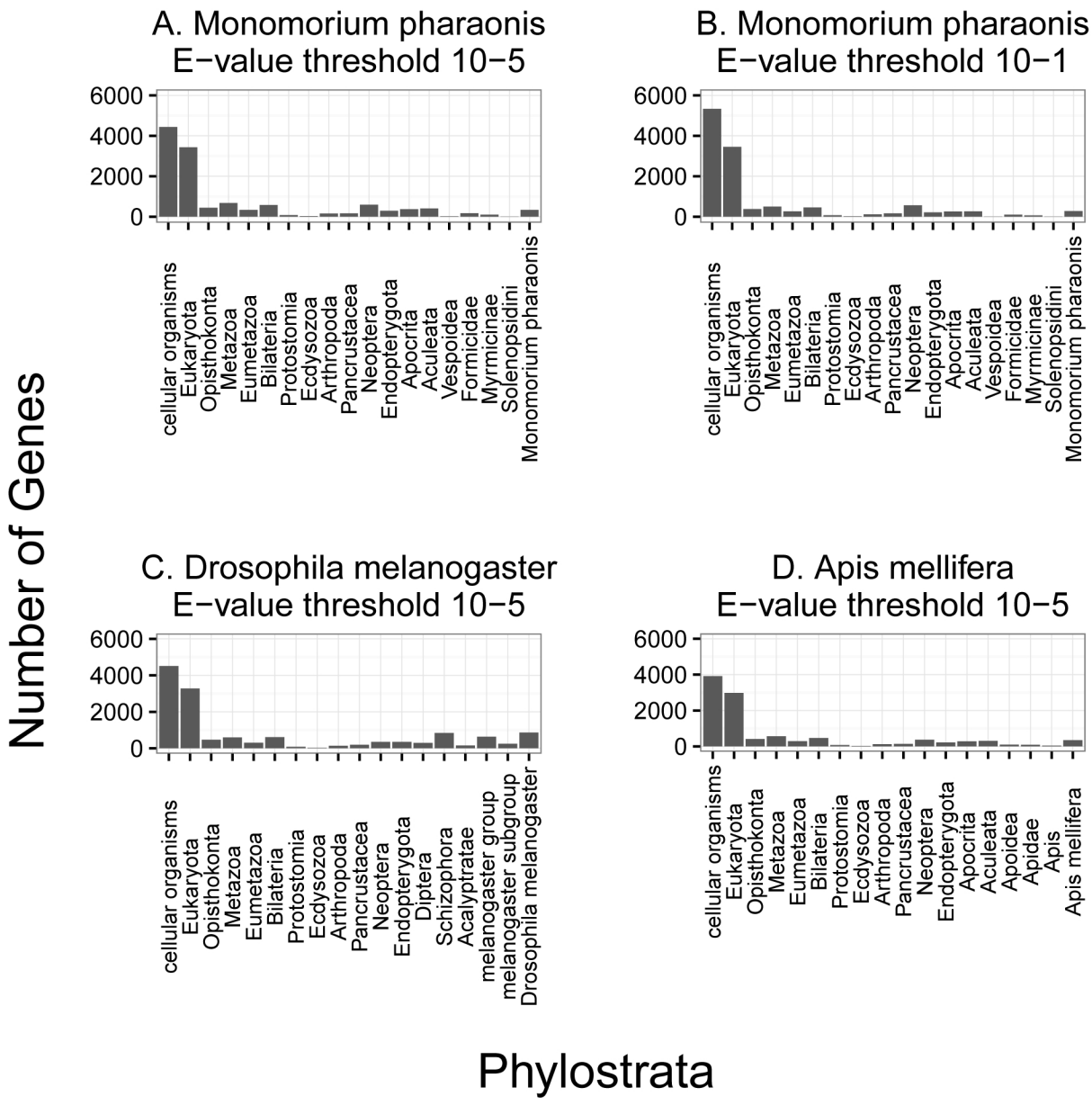

Figure S7

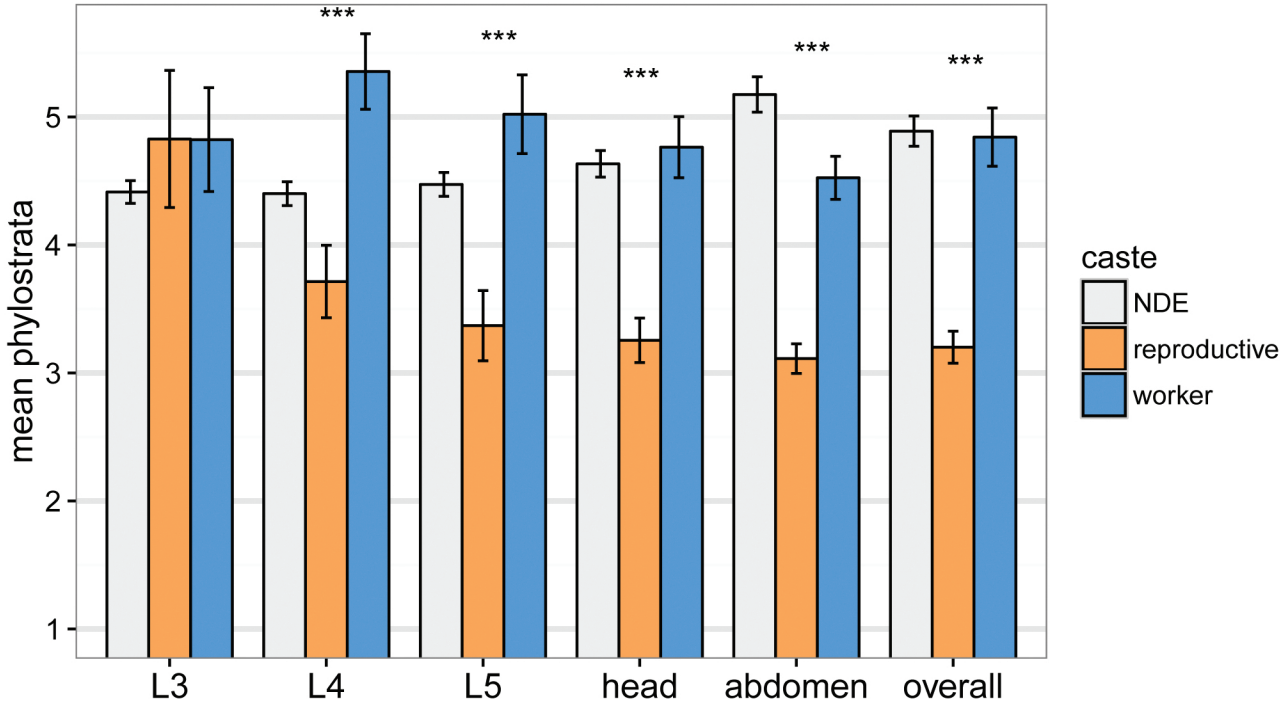

Figure S8

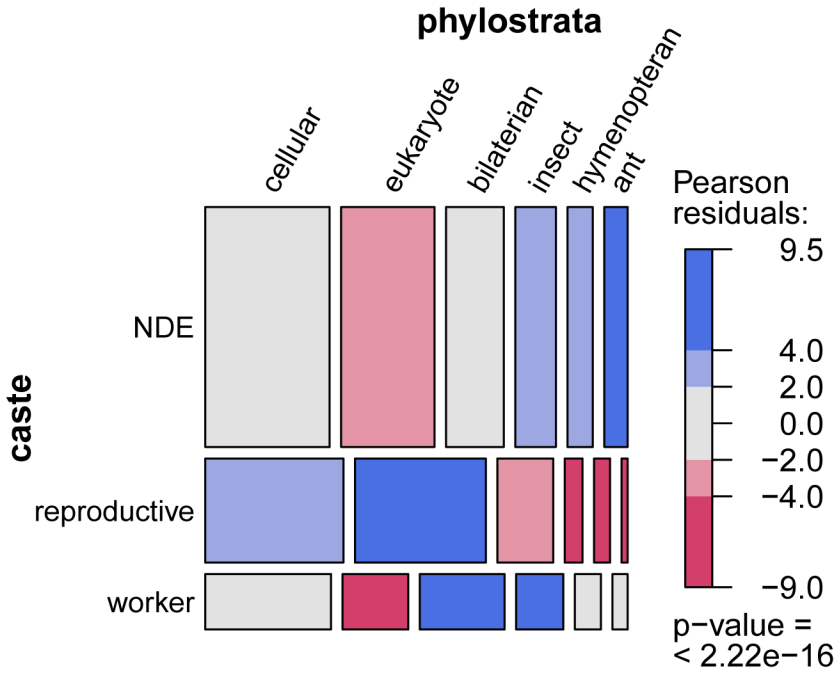

Figure S9

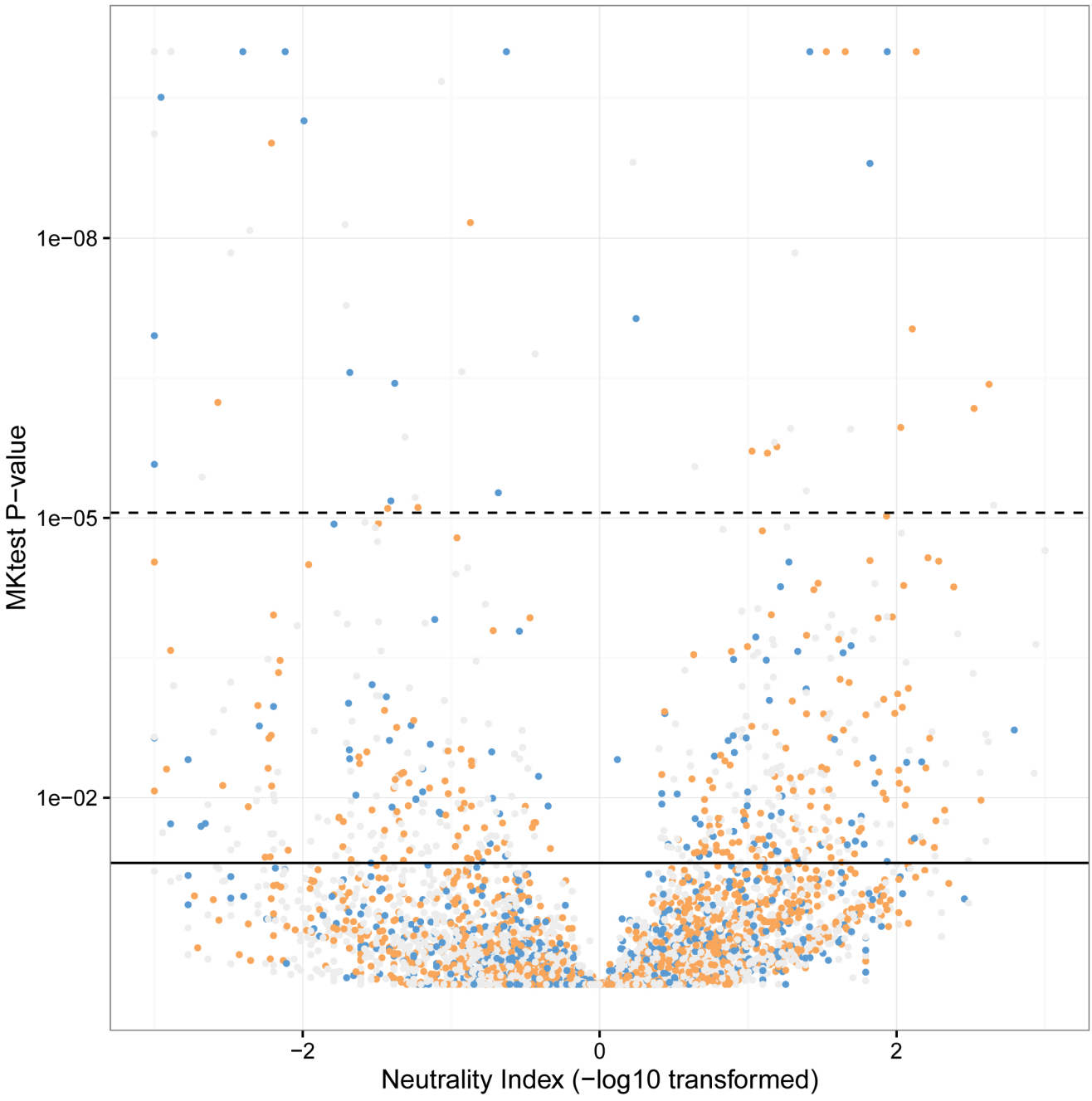

Figure S10

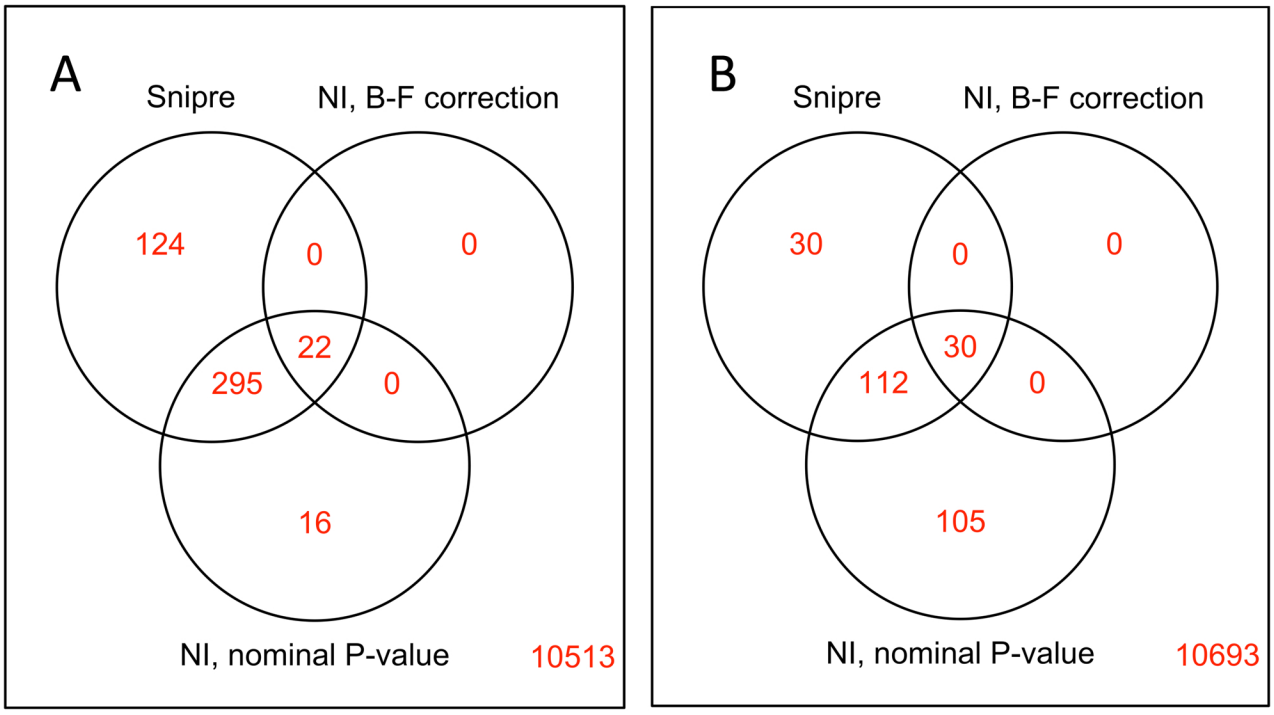

Table S1.

Samples included in the study. Stages (L1 - L5) refer to the developmental stage of the larvae sampled at the particular stage of sample collection (see Sampling Procedure). Adult queen samples are marked "Other" because they were collected separately.

Sample	Queen Presence	L1	L2	L3	L4	L5	Other	Total
Forager Head	Present	1	3	3	1	1	0	**9**
Forager Gaster	Present	2	2	3	2	2	0	**11**
Forager Head	Absent	2	3	3	3	2	0	**13**
Forager Gaster	Absent	2	3	2	3	2	0	**12**
Worker Nurse Head	Present	3	3	3	2	2	0	**13**
Worker Nurse Gaster	Present	3	3	3	3	2	0	**14**
Worker Nurse Head	Absent	2	3	2	2	3	0	**12**
Worker Nurse Gaster	Absent	3	2	3	2	3	0	**13**
Reproductive Nurse Head	Absent	0	2	2	2	3	0	**9**
Reproductive Nurse Gaster	Absent	0	3	3	3	3	0	**12**
Worker Larva	Present	0	3	3	3	3	0	**12**
Worker Larva	Absent	0	3	3	3	3	0	**12**
Reproductive Larva	Absent	0	3	3	3	3	0	**12**
Adult Queen Head	Present	0	0	0	0	0	3	**3**
Adult Queen Gaster	Absent	0	0	0	0	0	2	**2**

Table S2.

Top 20 worker-upregulated genes, sorted by FDR. Differential expression calculated using glm-like model including caste and developmental stage as fixed effects. Negative values of Log2 fold change indicate higher expression in worker samples.

Gene	Log2 Fold Change	P-Value	FDR	Description (SwissProt)
LOC105841041	-1.83	2.62E-32	3.19E-30	-
LOC105837944	-1.39	2.13E-26	1.67E-24	-
LOC105835450	-0.83	4.82E-26	3.62E-24	-
LOC105835451	-1.03	5.34E-23	2.96E-21	Endothelin-converting enzyme 1
LOC105834581	-1.09	1.82E-22	9.57E-21	TPPP family protein CG45057
LOC105832294	-2.01	3.58E-22	1.82E-20	Phospholipase A1
LOC105831727	-1.29	3.82E-22	1.93E-20	Ras-related protein Rab-3
LOC105836444	-1.16	2.31E-21	1.11E-19	Neurotrimin
LOC105831787	-1.11	3.56E-20	1.51E-18	Zinc finger protein 362
LOC105835899	-1.35	5.20E-19	1.95E-17	CUGBP Elav-like family member 4
LOC105835996	-1.03	2.32E-18	8.36E-17	Glutamate-gated chloride channel
LOC105831567	-1.61	8.58E-18	2.89E-16	Transcription factor 21
LOC105832152	-1.73	1.72E-17	5.59E-16	Esterase E4
LOC105837623	-1.26	5.68E-17	1.71E-15	Lachesin
LOC105832861	-1.28	9.58E-17	2.77E-15	-
LOC105837307	-0.89	1.00E-16	2.89E-15	Ankyrin-2
LOC105833207	-1.39	2.45E-16	6.83E-15	Pikachurin
LOC105829008	-4.29	8.32E-16	2.21E-14	-
LOC105830234	-2.91	8.34E-16	2.21E-14	-
LOC105830319	-4.11	8.73E-16	2.30E-14	-

Table S3.

Top 20 reproductive-upregulated genes, sorted by FDR. Positive values of Log2 fold change indicate higher expression in reproductive samples.

Gene	Log2 Fold Change	P-Value	FDR	Description (SwissProt)
LOC105837393	5.96	1.63E-143	1.79E-139	-
LOC105834006	4.27	7.02E-106	3.85E-102	Gephyrin
LOC105830579	3.92	1.02E-95	3.72E-92	Cytoplasmic polyadenylation element-binding protein 1
LOC105834706	5.08	1.76E-89	4.83E-86	Maternal effect protein oskar
LOC105835926	7.37	4.12E-87	9.03E-84	Vitellogenin-2
LOC105840630	10.61	4.49E-79	8.21E-76	-
LOC105840094	4.83	3.34E-71	5.24E-68	RCC1 and BTB domain-containing protein 1
LOC105831415	2.52	3.38E-68	4.64E-65	-
LOC105834586	2.56	2.40E-67	2.92E-64	Putative bifunctional UDP-N-acetylglucosamine transferase and deubiquitinase ALG13
LOC105828810	2.77	5.75E-65	6.30E-62	Gephyrin
LOC105829254	2.81	2.21E-63	2.20E-60	Maternal protein exuperantia
LOC105832526	2.21	1.97E-62	1.80E-59	Protein aubergine
LOC105830728	3.29	5.56E-62	4.69E-59	S-phase kinase-associated protein 2
LOC105833392	4.08	7.20E-62	5.64E-59	Poly(A) RNA polymerase gld-2 homolog A
LOC105828865	3.28	7.20E-60	5.27E-57	Hyaluronan mediated motility receptor
LOC105837552	3.97	6.20E-58	4.25E-55	Ribonuclease H1
LOC105829518	2.18	1.06E-57	6.81E-55	-
LOC105833500	2.19	9.12E-57	5.56E-54	Serine/threonine-protein kinase Chk2
LOC105838098	2.29	1.10E-56	6.37E-54	-
LOC105833023	3.33	1.49E-56	8.19E-54	-

Table S4.

Summary of the raw phylostrata identified for genes in the *M. pharoanis* genome (Fig. S6), and 6 categories that phylostrata were grouped into "Condensed PS1". For some analyses that required ~100 genes in each caste-associated category, we also created a third grouping, "Condensed PS2" that combined the hymenopteran and ant categories.

PS	Condensed PS1	Condensed PS2
cellular organisms	cellular	cellular
Eukaryota	eukaryote	eukaryote
Opisthokonta	bilaterian	bilaterian
Metazoa	bilaterian	bilaterian
Eumetazoa	bilaterian	bilaterian
Bilateria	bilaterian	bilaterian
Protostomia	bilaterian	bilaterian
Ecdysozoa	insect	insect
Arthropoda	insect	insect
Pancrustacea	insect	insect
Neoptera	insect	insect
Endopterygota	insect	insect
Apocrita	hymenopteran	hymenopteran
Aculeata	hymenopteran	hymenopteran
Vespoidea	hymenopteran	hymenopteran
Formicidae	ant	hymenopteran
Myrmicinae	ant	hymenopteran
Solenopsidini	ant	hymenopteran
Monomorium pharaonis	ant	hymenopteran

Table S5.

Top 3 GO terms for workers and reproductives for each differential expression test, as calculated using the R package GOstats, sorted by p-value. L2 not included due to paucity of differentially expressed genes.

GOBPID	Pvalue	OddsRatio	ExpCount	Count	Size	Term	Sample	Caste
GO:0006811	1.95E-12	3.554038863	26.99482536	63	154	ion transport	MainEffect	Worker
GO:0046034	3.35E-10	20.61047619	3.681112549	17	21	ATP metabolic process	MainEffect	Worker
GO:0007186	6.95E-10	3.66109831	19.10672704	46	109	G-protein coupled receptor signaling pathway	MainEffect	Worker
GO:0046483	4.38E-29	2.926335878	172.740621	287	567	heterocycle metabolic process	MainEffect	Reproductive
GO:0090304	1.36E-28	3.148458605	141.0562743	246	463	nucleic acid metabolic process	MainEffect	Reproductive
GO:1901360	2.19E-28	2.8789485	173.9592497	287	571	organic cyclic compound metabolic process	MainEffect	Reproductive
GO:0015711	0.000725545	5.986786787	1.629366106	7	22	organic anion transport	LarvalMain	Worker
GO:0015849	0.000725545	5.986786787	1.629366106	7	22	organic acid transport	LarvalMain	Worker
GO:0046942	0.000725545	5.986786787	1.629366106	7	22	carboxylic acid transport	LarvalMain	Worker
GO:1902578	1.28E-05	2.016145186	36.39068564	61	388	single-organism localization	LarvalMain	Reproductive
GO:0044699	1.45E-05	1.69630845	140.6856404	175	1500	single-organism process	LarvalMain	Reproductive
GO:0044765	1.58E-05	2.009181745	35.82794308	60	382	single-organism transport	LarvalMain	Reproductive
GO:0006040	1.24E-06	7.450946644	2.302716688	12	40	amino sugar metabolic process	L3	Worker
GO:0006030	1.24E-06	7.450946644	2.302716688	12	40	chitin metabolic process	L3	Worker
GO:1901071	1.24E-06	7.450946644	2.302716688	12	40	glucosamine-containing compound metabolic process	L3	Worker
GO:0006720	1.96E-05	14.98484848	0.626778784	6	17	isoprenoid metabolic process	L3	Reproductive
GO:0008299	1.96E-05	14.98484848	0.626778784	6	17	isoprenoid biosynthetic process	L3	Reproductive
GO:0044255	0.000359857	4.730458221	2.285899094	9	62	cellular lipid metabolic process	L3	Reproductive
GO:0007600	7.99E-12	5.110028653	11.4851229	37	92	sensory perception	L4	Worker
GO:0007606	7.99E-12	5.110028653	11.4851229	37	92	sensory perception of chemical stimulus	L4	Worker
GO:0003008	7.99E-12	5.110028653	11.4851229	37	92	system process	L4	Worker
GO:0044710	1.73E-09	2.068259836	82.89844761	130	671	single-organism metabolic process	L4	Reproductive
GO:0055114	1.23E-08	2.372507113	40.52263907	75	328	oxidation-reduction process	L4	Reproductive

GO:0005975	9.96E-06	2.690731282	15.44307891	33	125	carbohydrate metabolic process	L4	Reproductive
GO:0007608	3.27E-09	6.209081836	6.119340233	23	53	sensory perception of smell	L5	Worker
GO:0007600	6.01E-07	3.551861702	10.62225097	28	92	sensory perception	L5	Worker
GO:0007606	6.01E-07	3.551861702	10.62225097	28	92	sensory perception of chemical stimulus	L5	Worker
GO:0044710	2.09E-08	1.99925	78.3412031	121	671	single-organism metabolic process	L5	Reproductive
GO:0055114	7.45E-08	2.305735369	38.29495472	70	328	oxidation-reduction process	L5	Reproductive
GO:0008152	0.000452937	1.509656659	233.6225744	262	2001	metabolic process	L5	Reproductive
GO:0055114	1.70E-26	3.543282815	119.3402329	209	328	oxidation-reduction process	Gaster	Worker
GO:0044699	7.12E-15	1.788020026	545.76326	649	1500	single-organism process	Gaster	Worker
GO:0055085	3.98E-14	2.877425945	81.50064683	135	224	transmembrane transport	Gaster	Worker
GO:0044260	7.56E-57	3.762404675	279.5653299	469	952	cellular macromolecule metabolic process	Gaster	Reproductive
GO:0090304	1.66E-56	5.213744618	135.9650712	286	463	nucleic acid metabolic process	Gaster	Reproductive
GO:0006139	1.18E-48	4.196444744	159.7516171	307	544	nucleobase-containing compound metabolic process	Gaster	Reproductive
GO:0046034	2.31E-10	21.1920078	3.599611902	17	21	ATP metabolic process	Head	Worker
GO:0006163	2.16E-09	7.100674262	7.027813713	24	41	purine nucleotide metabolic process	Head	Worker
GO:0009161	2.77E-09	14.11695906	3.942432083	17	23	ribonucleoside monophosphate metabolic process	Head	Worker
GO:0006259	9.13E-09	3.252254768	22.91332471	49	108	DNA metabolic process	Head	Reproductive
GO:0044710	4.50E-07	1.657178803	142.3596378	190	671	single-organism metabolic process	Head	Reproductive
GO:0006950	1.40E-06	3.418803419	14.42690815	32	68	response to stress	Head	Reproductive

Table S6.

Top 3 GO terms for each phylostrata category for each differential expression test, as calculated using the R package GOstats, sorted by p-value. L2 not included due to paucity of differentially expressed genes. Missing phylostrata categories returned no significant GO terms.

GOBPID	Pvalue	OddsRatio	ExpCount	Count	Size	Term	Sample	Caste	Phylostrata
GO:0006811	6.23E-12	4.075406342	16.13712807	46	154	ion transport	MainEffect	Worker	cellular
GO:0044765	2.17E-11	2.73200443	40.02846054	81	382	single-organism transport	MainEffect	Worker	cellular
GO:0055085	2.20E-11	3.324968041	23.47218629	57	224	transmembrane transport	MainEffect	Worker	cellular
GO:0065007	1.16E-06	3.287946429	14.76746442	33	593	biological regulation	MainEffect	Worker	eukaryote
GO:0050789	2.40E-06	3.19417122	14.46862872	32	581	regulation of biological process	MainEffect	Worker	eukaryote
GO:0050794	5.66E-06	3.074883684	14.26940492	31	573	regulation of cellular process	MainEffect	Worker	eukaryote
GO:0007186	1.46E-26	21.5191793	3.243208279	33	109	G-protein coupled receptor signaling pathway	MainEffect	Worker	bilaterian
GO:0050794	1.41E-23	9.089912281	17.04915912	60	573	regulation of cellular process	MainEffect	Worker	bilaterian
GO:0050789	3.06E-23	8.921545106	17.28719276	60	581	regulation of biological process	MainEffect	Worker	bilaterian
GO:0006040	6.78E-05	61.78378378	0.090556274	3	40	amino sugar metabolic process	MainEffect	Worker	insect
GO:0006030	6.78E-05	61.78378378	0.090556274	3	40	chitin metabolic process	MainEffect	Worker	insect
GO:1901071	6.78E-05	61.78378378	0.090556274	3	40	glucosamine-containing compound metabolic process	MainEffect	Worker	insect
GO:0007600	5.91E-39	152.978836	1.130659767	29	92	sensory perception	MainEffect	Worker	hymenopteran_ant
GO:0007606	5.91E-39	152.978836	1.130659767	29	92	sensory perception of chemical stimulus	MainEffect	Worker	hymenopteran_ant
GO:0003008	5.91E-39	152.978836	1.130659767	29	92	system process	MainEffect	Worker	hymenopteran_ant
GO:0008152	7.43E-29	3.538233934	349.4631307	456	2001	metabolic process	MainEffect	Reproductive	cellular
GO:0044238	3.11E-15	2.120088457	250.4398448	333	1434	primary metabolic process	MainEffect	Reproductive	cellular
GO:0071704	1.53E-13	2.023948498	262.839586	340	1505	organic substance metabolic process	MainEffect	Reproductive	cellular

GO:0090304	9.66E-15	3.036420958	45.0721216	95	463	nucleic acid metabolic process	MainEffect	Reproductive	eukaryote
GO:0051649	2.92E-12	5.605050139	9.345407503	34	96	establishment of localization in cell	MainEffect	Reproductive	eukaryote
GO:0051641	7.52E-12	5.190694127	10.12419146	35	104	cellular localization	MainEffect	Reproductive	eukaryote
GO:0031323	3.77E-17	9.529559748	5.68305304	32	191	regulation of cellular metabolic process	MainEffect	Reproductive	bilaterian
GO:0019222	1.56E-16	8.99047619	5.95084088	32	200	regulation of metabolic process	MainEffect	Reproductive	bilaterian
GO:0060255	2.58E-16	9.141108114	5.623544631	31	189	regulation of macromolecule metabolic process	MainEffect	Reproductive	bilaterian
GO:0007600	5.64E-10	123.4470588	0.26778784	7	92	sensory perception	MainEffect	Reproductive	hymenopteran_ant
GO:0007606	5.64E-10	123.4470588	0.26778784	7	92	sensory perception of chemical stimulus	MainEffect	Reproductive	hymenopteran_ant
GO:0003008	5.64E-10	123.4470588	0.26778784	7	92	system process	MainEffect	Reproductive	hymenopteran_ant
GO:0006811	1.39E-05	3.35645933	7.620310479	21	154	ion transport	LarvalMain	Worker	cellular
GO:0006508	0.000148191	2.454297821	13.01390686	27	263	proteolysis	LarvalMain	Worker	cellular
GO:0006820	0.000277076	5.735960591	1.781371281	8	36	anion transport	LarvalMain	Worker	cellular
GO:0065007	0.000350266	4.004145078	5.561772316	14	593	biological regulation	LarvalMain	Worker	eukaryote
GO:0007165	0.000783482	4.257379353	3.254527814	10	347	signal transduction	LarvalMain	Worker	eukaryote
GO:0044700	0.000820369	4.229156963	3.273285899	10	349	single organism signaling	LarvalMain	Worker	eukaryote
GO:0050794	4.20E-12	10.33104396	7.227360931	27	573	regulation of cellular process	LarvalMain	Worker	bilaterian
GO:0050789	5.93E-12	10.14936823	7.328266494	27	581	regulation of biological process	LarvalMain	Worker	bilaterian
GO:0065007	9.88E-12	9.886484099	7.479624838	27	593	biological regulation	LarvalMain	Worker	bilaterian

GO:0006040	0.025709996	78.23076923	0.025873221	1	40	amino sugar metabolic process	LarvalMain	Worker	insect
GO:0006030	0.025709996	78.23076923	0.025873221	1	40	chitin metabolic process	LarvalMain	Worker	insect
GO:1901071	0.025709996	78.23076923	0.025873221	1	40	glucosamine-containing compound metabolic process	LarvalMain	Worker	insect
GO:0055085	1.46E-06	2.87593985	14.63389392	34	224	transmembrane transport	LarvalMain	Reproductive	cellular
GO:0044710	3.85E-06	2.068575064	43.83635188	71	671	single-organism metabolic process	LarvalMain	Reproductive	cellular
GO:0055114	9.66E-05	2.153374233	21.42820181	39	328	oxidation-reduction process	LarvalMain	Reproductive	cellular
GO:0006281	2.68E-05	9.741395349	0.921733506	7	57	DNA repair	LarvalMain	Reproductive	eukaryote
GO:0006974	3.38E-05	9.360465116	0.954075032	7	59	cellular response to DNA damage stimulus	LarvalMain	Reproductive	eukaryote
GO:0033554	3.78E-05	9.180781044	0.970245796	7	60	cellular response to stress	LarvalMain	Reproductive	eukaryote
GO:0006869	3.01E-11	111.3072917	0.150388098	7	15	lipid transport	LarvalMain	Reproductive	bilaterian
GO:0010876	3.01E-11	111.3072917	0.150388098	7	15	lipid localization	LarvalMain	Reproductive	bilaterian
GO:0033036	1.54E-05	11.00949367	0.862225097	7	86	macromolecule localization	LarvalMain	Reproductive	bilaterian
GO:0007600	2.40E-05	45.40909091	0.208279431	4	92	sensory perception	LarvalMain	Reproductive	hymenopteran_ant
GO:0007606	2.40E-05	45.40909091	0.208279431	4	92	sensory perception of chemical stimulus	LarvalMain	Reproductive	hymenopteran_ant
GO:0003008	2.40E-05	45.40909091	0.208279431	4	92	system process	LarvalMain	Reproductive	hymenopteran_ant
GO:0044765	6.83E-06	2.752626552	15.19598965	33	382	single-organism transport	L3	Worker	cellular
GO:1902578	9.64E-06	2.699906103	15.43467012	33	388	single-organism localization	L3	Worker	cellular
GO:0055114	1.86E-05	2.754927773	13.04786546	29	328	oxidation-reduction process	L3	Worker	cellular

GO:0030328	0.004204398	Inf	0.004204398	1	1	prenylcysteine catabolic process	L3	Worker	eukaryote
GO:0000098	0.004204398	Inf	0.004204398	1	1	sulfur amino acid catabolic process	L3	Worker	eukaryote
GO:0030329	0.004204398	Inf	0.004204398	1	1	prenylcysteine metabolic process	L3	Worker	eukaryote
GO:0007186	4.68E-08	14.24723425	1.092820181	10	109	G-protein coupled receptor signaling pathway	L3	Worker	bilaterian
GO:0050794	9.65E-07	6.251975052	5.744825356	18	573	regulation of cellular process	L3	Worker	bilaterian
GO:0050789	1.20E-06	6.143462222	5.825032342	18	581	regulation of biological process	L3	Worker	bilaterian
GO:0006040	5.78E-09	217.8571429	0.090556274	5	40	amino sugar metabolic process	L3	Worker	insect
GO:0006030	5.78E-09	217.8571429	0.090556274	5	40	chitin metabolic process	L3	Worker	insect
GO:1901071	5.78E-09	217.8571429	0.090556274	5	40	glucosamine-containing compound metabolic process	L3	Worker	insect
GO:0050909	0.012613195	Inf	0.012613195	1	39	sensory perception of taste	L3	Worker	hymenopteran_ant
GO:0007600	0.029754204	Inf	0.029754204	1	92	sensory perception	L3	Worker	hymenopteran_ant
GO:0007606	0.029754204	Inf	0.029754204	1	92	sensory perception of chemical stimulus	L3	Worker	hymenopteran_ant
GO:0006720	4.38E-05	17.1347032	0.428848642	5	17	isoprenoid metabolic process	L3	Reproductive	cellular
GO:0008299	4.38E-05	17.1347032	0.428848642	5	17	isoprenoid biosynthetic process	L3	Reproductive	cellular
GO:0044255	0.000128384	6.264550265	1.564036223	8	62	cellular lipid metabolic process	L3	Reproductive	cellular
GO:0010970	0.005174644	Inf	0.005174644	1	1	establishment of localization by movement along microtubule	L3	Reproductive	eukaryote
GO:0098840	0.005174644	Inf	0.005174644	1	1	protein transport along microtubule	L3	Reproductive	eukaryote
GO:0042073	0.005174644	Inf	0.005174644	1	1	intraciliary transport	L3	Reproductive	eukaryote

GO:0050794	9.40E-06	20.08244681	2.038486417	9	573	regulation of cellular process	L3	Reproductive	bilaterian
GO:0050789	1.06E-05	19.73863636	2.06694696	9	581	regulation of biological process	L3	Reproductive	bilaterian
GO:0065007	1.26E-05	19.24058219	2.109637775	9	593	biological regulation	L3	Reproductive	bilaterian
GO:0007600	2.40E-06	43.04597701	0.26778784	5	92	sensory perception	L3	Reproductive	hymenopteran_ant
GO:0007606	2.40E-06	43.04597701	0.26778784	5	92	sensory perception of chemical stimulus	L3	Reproductive	hymenopteran_ant
GO:0003008	2.40E-06	43.04597701	0.26778784	5	92	system process	L3	Reproductive	hymenopteran_ant
GO:0006508	7.18E-09	3.162303099	18.11739974	44	263	proteolysis	L4	Worker	cellular
GO:0006811	3.41E-06	3.145542291	10.60866753	27	154	ion transport	L4	Worker	cellular
GO:0055114	3.00E-05	2.226843332	22.59508409	42	328	oxidation-reduction process	L4	Worker	cellular
GO:0065007	9.05E-11	5.535394265	12.08247089	35	593	biological regulation	L4	Worker	eukaryote
GO:0050789	1.43E-09	4.980109489	11.83796895	33	581	regulation of biological process	L4	Worker	eukaryote
GO:0050794	4.85E-09	4.747242263	11.67496766	32	573	regulation of cellular process	L4	Worker	eukaryote
GO:0050794	4.03E-19	11.27285115	11.30433376	43	573	regulation of cellular process	L4	Worker	bilaterian
GO:0050789	7.08E-19	11.0697026	11.46216041	43	581	regulation of biological process	L4	Worker	bilaterian
GO:0065007	1.62E-18	10.77606061	11.69890039	43	593	biological regulation	L4	Worker	bilaterian
GO:0007600	1.37E-51	274.8673469	1.279430789	36	92	sensory perception	L4	Worker	hymenopteran_ant
GO:0007606	1.37E-51	274.8673469	1.279430789	36	92	sensory perception of chemical stimulus	L4	Worker	hymenopteran_ant
GO:0003008	1.37E-51	274.8673469	1.279430789	36	92	system process	L4	Worker	hymenopteran_ant
GO:0044710	2.90E-13	2.638315484	63.1503881	115	671	single-organism metabolic process	L4	Reproductive	cellular
GO:0055114	2.52E-12	3.121996562	30.86934023	70	328	oxidation-reduction process	L4	Reproductive	cellular
GO:0008152	3.63E-09	2.293970547	188.3217982	232	2001	metabolic process	L4	Reproductive	cellular

GO:0006810	0.002909657	2.793736501	6.479301423	14	477	transport	L4	Reproductive	eukaryote
GO:0051234	0.003089857	2.772532189	6.520051746	14	480	establishment of localization	L4	Reproductive	eukaryote
GO:0051179	0.003687396	2.710526316	6.642302717	14	489	localization	L4	Reproductive	eukaryote
GO:0006869	1.81E-12	112.2949309	0.18919793	8	15	lipid transport	L4	Reproductive	bilaterian
GO:0010876	1.81E-12	112.2949309	0.18919793	8	15	lipid localization	L4	Reproductive	bilaterian
GO:0033036	7.86E-06	9.842845327	1.084734799	8	86	macromolecule localization	L4	Reproductive	bilaterian
GO:0006040	1.19E-07	339	0.064683053	4	40	amino sugar metabolic process	L4	Reproductive	insect
GO:0006030	1.19E-07	339	0.064683053	4	40	chitin metabolic process	L4	Reproductive	insect
GO:1901071	1.19E-07	339	0.064683053	4	40	glucosamine-containing compound metabolic process	L4	Reproductive	insect
GO:0007600	9.98E-05	101.0898876	0.119016818	3	92	sensory perception	L4	Reproductive	hymenopteran_ant
GO:0007606	9.98E-05	101.0898876	0.119016818	3	92	sensory perception of chemical stimulus	L4	Reproductive	hymenopteran_ant
GO:0003008	9.98E-05	101.0898876	0.119016818	3	92	system process	L4	Reproductive	hymenopteran_ant
GO:0055114	4.19E-08	2.723857659	23.97412678	51	328	oxidation-reduction process	L5	Worker	cellular
GO:0006508	7.65E-06	2.459845302	19.22315653	39	263	proteolysis	L5	Worker	cellular
GO:0006811	8.94E-05	2.638937097	11.25614489	25	154	ion transport	L5	Worker	cellular
GO:0065007	2.52E-10	6.7114595	9.205692109	29	593	biological regulation	L5	Worker	eukaryote
GO:0050789	9.91E-10	6.306329114	9.019404916	28	581	regulation of biological process	L5	Worker	eukaryote
GO:0050794	4.39E-09	5.882260597	8.895213454	27	573	regulation of cellular process	L5	Worker	eukaryote
GO:0050794	1.83E-13	10.65023374	7.968628719	30	573	regulation of cellular process	L5	Worker	bilaterian
GO:0050789	2.70E-13	10.46209689	8.079883571	30	581	regulation of biological process	L5	Worker	bilaterian
GO:0065007	4.77E-13	10.18991666	8.246765847	30	593	biological regulation	L5	Worker	bilaterian

GO:0006040	0.025709996	78.23076923	0.025873221	1	40	amino sugar metabolic process	L5	Worker	insect
GO:0006030	0.025709996	78.23076923	0.025873221	1	40	chitin metabolic process	L5	Worker	insect
GO:1901071	0.025709996	78.23076923	0.025873221	1	40	glucosamine-containing compound metabolic process	L5	Worker	insect
GO:0007600	4.56E-37	177.6065934	1.01164295	27	92	sensory perception	L5	Worker	hymenopteran_ant
GO:0007606	4.56E-37	177.6065934	1.01164295	27	92	sensory perception of chemical stimulus	L5	Worker	hymenopteran_ant
GO:0003008	4.56E-37	177.6065934	1.01164295	27	92	system process	L5	Worker	hymenopteran_ant
GO:0044710	2.40E-13	2.754534915	57.0740621	107	671	single-organism metabolic process	L5	Reproductive	cellular
GO:0055114	4.46E-13	3.363359137	27.89909444	67	328	oxidation-reduction process	L5	Reproductive	cellular
GO:0008152	1.75E-08	2.296387598	170.2014877	210	2001	metabolic process	L5	Reproductive	cellular
GO:0051649	0.000343296	5.356363636	1.800776197	8	96	establishment of localization in cell	L5	Reproductive	eukaryote
GO:0022406	0.000485846	27.52727273	0.168822768	3	9	membrane docking	L5	Reproductive	eukaryote
GO:0051641	0.000593227	4.896666667	1.95084088	8	104	cellular localization	L5	Reproductive	eukaryote
GO:0006869	1.05E-05	41.07744108	0.150388098	4	15	lipid transport	L5	Reproductive	bilaterian
GO:0010876	1.05E-05	41.07744108	0.150388098	4	15	lipid localization	L5	Reproductive	bilaterian
GO:0050794	0.000569083	3.685993897	5.744825356	14	573	regulation of cellular process	L5	Reproductive	bilaterian
GO:0006040	2.01E-06	Inf	0.038809832	3	40	amino sugar metabolic process	L5	Reproductive	insect

GO:0006030	2.01E-06	Inf	0.038809832	3	40	chitin metabolic process	L5	Reproductive	insect
GO:1901071	2.01E-06	Inf	0.038809832	3	40	glucosamine-containing compound metabolic process	L5	Reproductive	insect
GO:0007600	0.000244237	50.52808989	0.148771022	3	92	sensory perception	L5	Reproductive	hymenopteran_ant
GO:0007606	0.000244237	50.52808989	0.148771022	3	92	sensory perception of chemical stimulus	L5	Reproductive	hymenopteran_ant
GO:0003008	0.000244237	50.52808989	0.148771022	3	92	system process	L5	Reproductive	hymenopteran_ant
GO:0055114	5.29E-45	5.51156392	81.57567917	194	328	oxidation-reduction process	Gaster	Worker	cellular
GO:0044710	3.59E-28	2.829303501	166.8819534	280	671	single-organism metabolic process	Gaster	Worker	cellular
GO:0055085	7.96E-18	3.432707097	55.71021992	113	224	transmembrane transport	Gaster	Worker	cellular
GO:0015991	5.34E-07	44.71212121	0.401681759	6	9	ATP hydrolysis coupled proton transport	Gaster	Worker	eukaryote
GO:0015988	5.34E-07	44.71212121	0.401681759	6	9	energy coupled proton transmembrane transport, against electrochemical gradient	Gaster	Worker	eukaryote
GO:0090662	5.34E-07	44.71212121	0.401681759	6	9	ATP hydrolysis coupled transmembrane transport	Gaster	Worker	eukaryote
GO:0007186	4.14E-34	20.91978093	5.005821475	45	109	G-protein coupled receptor signaling pathway	Gaster	Worker	bilaterian
GO:0050794	3.55E-30	7.766867116	26.31500647	86	573	regulation of cellular process	Gaster	Worker	bilaterian
GO:0065007	7.35E-30	7.640244341	27.23350582	87	593	biological regulation	Gaster	Worker	bilaterian
GO:0006040	3.91E-05	82.40540541	0.077619664	3	40	amino sugar metabolic process	Gaster	Worker	insect
GO:0006030	3.91E-05	82.40540541	0.077619664	3	40	chitin metabolic process	Gaster	Worker	insect
GO:1901071	3.91E-05	82.40540541	0.077619664	3	40	glucosamine-containing compound metabolic process	Gaster	Worker	insect
GO:0007600	2.83E-72	265.3066202	1.934023286	51	92	sensory perception	Gaster	Worker	hymenopteran_ant
GO:0007606	2.83E-72	265.3066202	1.934023286	51	92	sensory perception of chemical stimulus	Gaster	Worker	hymenopteran_ant

GO:0003008	2.83E-72	265.3066202	1.934023286	51	92	system process	Gaster	Worker	hymenopteran_ant
GO:0044237	3.95E-32	3.340921765	174.6005821	290	1161	cellular metabolic process	Gaster	Reproductive	cellular
GO:0044260	6.29E-32	3.362369338	143.1694696	255	952	cellular macromolecule metabolic process	Gaster	Reproductive	cellular
GO:0044238	2.96E-26	2.997337956	215.656533	320	1434	primary metabolic process	Gaster	Reproductive	cellular
GO:0090304	2.39E-24	3.851938105	52.70892626	124	463	nucleic acid metabolic process	Gaster	Reproductive	eukaryote
GO:0016070	2.38E-19	3.639424649	41.55239327	99	365	RNA metabolic process	Gaster	Reproductive	eukaryote
GO:0006139	4.54E-18	3.050319094	61.9301423	125	544	nucleobase-containing compound metabolic process	Gaster	Reproductive	eukaryote
GO:0050794	4.03E-15	6.162917195	15.3813066	47	573	regulation of cellular process	Gaster	Reproductive	bilaterian
GO:0050789	7.11E-15	6.051029963	15.59605433	47	581	regulation of biological process	Gaster	Reproductive	bilaterian
GO:0065007	1.63E-14	5.889346764	15.91817594	47	593	biological regulation	Gaster	Reproductive	bilaterian
GO:0007591	0.000323415	Inf	0.000323415	1	1	molting cycle, chitin-based cuticle	Gaster	Reproductive	insect
GO:0018990	0.000323415	Inf	0.000323415	1	1	ecdysis, chitin-based cuticle	Gaster	Reproductive	insect
GO:0022404	0.000323415	Inf	0.000323415	1	1	molting cycle process	Gaster	Reproductive	insect
GO:0007608	9.18E-05	60.72	0.102846054	3	53	sensory perception of smell	Gaster	Reproductive	hymenopteran_ant
GO:0007600	0.000477944	33.6741573	0.178525226	3	92	sensory perception	Gaster	Reproductive	hymenopteran_ant
GO:0007606	0.000477944	33.6741573	0.178525226	3	92	sensory perception of chemical stimulus	Gaster	Reproductive	hymenopteran_ant
GO:0044765	1.70E-11	2.784824172	38.42238034	79	382	single-organism transport	Head	Worker	cellular

GO:1902578	3.97E-11	2.724137931	39.02587322	79	388	single-organism localization	Head	Worker	cellular
GO:0006836	3.03E-10	37.1638796	1.508732212	12	15	neurotransmitter transport	Head	Worker	cellular
GO:0050789	7.05E-08	3.619816514	15.2202458	36	581	regulation of biological process	Head	Worker	eukaryote
GO:0065007	1.22E-07	3.52459605	15.53460543	36	593	biological regulation	Head	Worker	eukaryote
GO:0050794	6.18E-07	3.317727865	15.0106727	34	573	regulation of cellular process	Head	Worker	eukaryote
GO:0007186	1.59E-27	25.41125541	2.820181113	32	109	G-protein coupled receptor signaling pathway	Head	Worker	bilaterian
GO:0050794	2.26E-22	9.976433971	14.82535576	54	573	regulation of cellular process	Head	Worker	bilaterian
GO:0050789	4.58E-22	9.793460809	15.03234153	54	581	regulation of biological process	Head	Worker	bilaterian
GO:0006040	2.59E-10	179.3529412	0.116429495	6	40	amino sugar metabolic process	Head	Worker	insect
GO:0006030	2.59E-10	179.3529412	0.116429495	6	40	chitin metabolic process	Head	Worker	insect
GO:1901071	2.59E-10	179.3529412	0.116429495	6	40	glucosamine-containing compound metabolic process	Head	Worker	insect
GO:0007600	3.24E-49	229.6491228	1.279430789	35	92	sensory perception	Head	Worker	hymenopteran_ant
GO:0007606	3.24E-49	229.6491228	1.279430789	35	92	sensory perception of chemical stimulus	Head	Worker	hymenopteran_ant
GO:0003008	3.24E-49	229.6491228	1.279430789	35	92	system process	Head	Worker	hymenopteran_ant
GO:0008152	6.79E-27	4.180646933	262.097348	352	2001	metabolic process	Head	Reproductive	cellular
GO:0044710	3.33E-15	2.509660566	87.88971539	152	671	single-organism metabolic process	Head	Reproductive	cellular
GO:0055114	1.44E-08	2.325211009	42.96248383	78	328	oxidation-reduction process	Head	Reproductive	cellular
GO:0007017	1.05E-07	8.821647059	2.249029754	13	38	microtubule-based process	Head	Reproductive	eukaryote
GO:0006259	7.08E-07	4.204767986	6.391979301	21	108	DNA metabolic process	Head	Reproductive	eukaryote
GO:0033554	1.09E-06	5.682539683	3.551099612	15	60	cellular response to stress	Head	Reproductive	eukaryote
GO:0065007	5.29E-08	4.252502224	12.08247089	31	593	biological regulation	Head	Reproductive	bilaterian

GO:0050789	1.38E-07	4.088434252	11.83796895	30	581	regulation of biological process	Head	Reproductive	bilaterian
GO:0050794	4.08E-07	3.896247837	11.67496766	29	573	regulation of cellular process	Head	Reproductive	bilaterian
GO:0048598	0.001293661	Inf	0.001293661	1	1	embryonic morphogenesis	Head	Reproductive	hymenopteran_ant
GO:0035434	0.003877217	514.3333333	0.003880983	1	3	copper ion transmembrane transport	Head	Reproductive	hymenopteran_ant
GO:0009790	0.003877217	514.3333333	0.003880983	1	3	embryo development	Head	Reproductive	hymenopteran_ant

Table S7.

Model selection parameters from MKtest2.0 (*13, 14*) for estimating *α*, the proportion of amino acid substitution driven by positive selection. The first three columns show the number of parameters for *α* and *f*, as well as the total number of model parameters, *K*. We mainly considered models with per-class estimates (i.e. three separate estimates for worker-associated, reproductive-associated, and NDE genes) for both *α* and *f*, or with per-locus estimates for *f*. Of these two main models in bold that we considered, the model including per-locus estimates of *f* fit the data much better. We focus on results from this model, although the per-class *α* and *f* model produced very similar results, showing the same pattern and overlapping *α* estimates. We also show results from models where *α* and/or *f* is fixed or had a single, genome-wide estimate. LnL maximized log likelihood; AIC, Akaike information criterion; AICc, second-order AIC; BIC, Bayesian information criterion (Welch 2006; Obbard et al. 2009).

Model description	***α***	***f***	***K***	***LnL***	**AIC**	**AICc**	**BIC**
	0	0	2	-1002096.22231	2004196.44462	2004196.44495	2004213.43161
	3	0	5	-678989.00409	1357988.00818	1357988.00984	1358030.4765
	1	0	3	-615656.376167	1231318.75233	1231318.753	1231344.23282
	0	1	3	-522404.908371	1044815.81674	1044815.81741	1044841.29722
	1	1	4	-521956.917522	1043921.83504	1043921.83615	1043955.80902
	1	3	6	-521585.629106	1043183.25821	1043183.26054	1043234.21918
	3	1	6	-521394.185871	1042800.37174	1042800.37407	1042851.33271
Per-class α and f	**3**	**3**	**8**	**-521349.0028**	**1042714.0056**	**1042714.00959**	**1042781.95355**
	0	9020	9022	-378721.983142	775487.966284	781505.300505	852116.268919
	1	9020	9023	-377650.16441	773346.32882	779365.219417	849983.124949
Per-class α and per-locus f	**3**	**9020**	**9025**	**-377432.859261**	**772917.718522**	**778937/722662**	**849569.501639**

Table S8.

Top 20 positively selected genes (sorted by p-value of McDonald-Kreitman test) for reproductive- and worker-associated genes. SnIPRE.class is the selection categories as calculated by SnIPRE. "NI.class" refers to selection categories, as calculated using a combination of the neutrality index and the P-value from the McDonald-Kreitman test. Genes with negative values of -log10(Neutrality Index) and p-values less than 0.05 are defined as under purifying selection, while such genes with positive -log10(Neutrality Index) values are assigned to the positive selection category. "NI.class B-F correction" uses the same method but the p-value cutoff from the McDonald-Kreitman test is adjusted for multiple comparisons using the Bonferroni procedure.

Gene	Snipre. class	NI.class	NI.class (B-F correction)	Gamma	Neutrality Index (-Log10 tranformed)	MK P-value	Description (SwissProt)	Description (UniProt)	Caste
LOC105832526	pos	pos	pos	5.94	2.13	8.70E-15	Protein aubergine	Piwi-like protein	Reproductive
LOC105828570	pos	pos	pos	3.24	1.53	3.76E-12	ABC transporter G family member 20	ABC transporter G family member 20 (Fragment)	Reproductive
LOC105829311	pos	pos	pos	5.53	2.52	6.69E-07	Probable ATP-dependent RNA helicase spindle-E	Putative ATP-dependent RNA helicase TDRD9	Reproductive
LOC105836534	pos	pos	pos	2.43	1.29	1.10E-06	Probable multidrug resistance-associated protein lethal(2)03659	Putative multidrug resistance-associated protein lethal(2)03659	Reproductive
LOC105830831	pos	pos	pos	2.22	1.18	1.54E-06	Transient receptor potential cation channel subfamily V member 5	Putative uncharacterized protein (Fragment)	Reproductive
LOC105831051	pos	pos	pos	2.05	1.13	2.02E-06	Venom serine protease Bi-VSP	Uncharacterized protein	Reproductive
LOC105831878	pos	pos	neut	4.05	2.21	2.67E-05	Adenylate cyclase type 8	Uncharacterized protein	Reproductive
LOC105833310	pos	pos	neut	3.54	1.82	2.86E-05	Structural maintenance of	Structural maintenance of	Reproductive

							chromosomes protein 5	chromosomes protein 5	
LOC105835371	pos	pos	neut	4.34	2.28	2.91E-05	Major facilitator superfamily domain-containing protein 6	Major facilitator superfamily domain-containing protein 6 (Fragment)	Reproductive
LOC105828996	pos	pos	neut	3.46	2.38	5.48E-05	-	-	Reproductive
LOC105832368	pos	pos	neut	1.97	1.16	0.000109 152	Biotin--protein ligase	Biotin--protein ligase (Fragment)	Reproductive
LOC105840269	pos	pos	neut	4.02	2.01	0.000771 347	-	Putative uncharacterized protein (Fragment)	Reproductive
LOC105833118	pos	pos	neut	1.74	1.12	0.003593 458	Serine/threonine-protein kinase SIK2	Uncharacterized protein	Reproductive
LOC105837631	pos	pos	neut	1.32	0.84	0.004018 889	Luciferin 4-monooxygenase	Luciferin 4-monooxygenase	Reproductive
LOC105837563	pos	pos	neut	1.46	0.88	0.004464 27	Probable multidrug resistance-associated protein lethal(2)03659	Multidrug resistance-associated protein 4	Reproductive
LOC105830185	pos	pos	neut	2.08	1.43	0.005106 672	-	Putative uncharacterized protein	Reproductive
LOC105835393	pos	pos	neut	2.33	1.88	0.005291 519	Serine protease snake	Serine protease snake	Reproductive
LOC105830282	pos	pos	neut	0.61	0.42	0.005630 685	Lymphoid-restricted membrane protein	Protein SAAL1 (Fragment)	Reproductive
LOC105835118	pos	pos	neut	1.78	1.35	0.005987 065	-	Putative uncharacterized protein (Fragment)	Reproductive

LOC105837746	pos	pos	neut	1.10	0.74	0.006518212	ATP-binding cassette sub-family A member 13	ATP-binding cassette sub-family A member 13	Reproductive
LOC105833674	pos	pos	pos	4.99	1.94	1.44E-14	Voltage-dependent calcium channel type A subunit alpha-1	Voltage dependent Ca2 channel Cav2 subunit	Worker
LOC105835213	pos	pos	pos	3.01	1.42	7.85E-12	Protein unc-79 homolog	Uncharacterized protein	Worker
LOC105837842	pos	pos	pos	4.23	1.82	1.58E-09	Sodium-independent sulfate anion transporter	Sodium-independent sulfate anion transporter	Worker
LOC105832885	pos	pos	neut	2.33	1.27	2.97E-05	Talin-1	Talin-1	Worker
LOC105835926	pos	pos	neut	2.66	1.61	0.000200458	Vitellogenin-2	Putative uncharacterized protein (Fragment)	Worker
LOC105840699	pos	pos	neut	2.03	1.17	0.000508296	Vitamin K-dependent gamma-carboxylase	Uncharacterized protein	Worker
LOC105837307	pos	pos	neut	0.66	0.44	0.001247 57	Ankyrin-2	Putative uncharacterized protein (Fragment)	Worker
LOC105838219	pos	pos	neut	3.38	2.79	0.001877545	Glutamate receptor ionotropic kainate 2	Glutamate receptor ionotropic kainate 2	Worker
LOC105836662	pos	pos	neut	1.51	0.96	0.002224554	Protein phosphatase 1E	Protein phosphatase 1F	Worker
LOC105831090	pos	pos	neut	2.83	2.08	0.003082822	Dipeptidyl peptidase 3	Putative uncharacterized protein (Fragment)	Worker

LOC105837460	pos	pos	neut	1.32	0.78	0.005261444	-	Putative uncharacterized protein	Worker
LOC105834708	pos	pos	neut	1.73	1.16	0.005502118	Glucose dehydrogenase FAD quinone	Uncharacterized protein	Worker
LOC105837257	pos	pos	neut	1.54	0.99	0.012181701	Periaxin	Putative uncharacterized protein	Worker
LOC105837961	pos	pos	neut	1.46	0.97	0.014182719	Protein disconnected	Putative uncharacterized protein (Fragment)	Worker
LOC105828589	pos	pos	neut	1.74	1.22	0.014358752	Harmonin	Uncharacterized protein	Worker
LOC105832072	pos	pos	neut	1.56	1.16	0.015659886	-	Putative uncharacterized protein	Worker
LOC105829245	pos	pos	neut	2.43	1.76	0.015757911	Discoidin domain-containing receptor 2	Putative uncharacterized protein (Fragment)	Worker
LOC105835954	pos	pos	neut	1.03	0.64	0.016746237	SH3 and multiple ankyrin repeat domains protein 3	SH3 and multiple ankyrin repeat domains protein 3	Worker
LOC105840696	pos	pos	neut	1.97	1.21	0.017236477	Cytochrome P450 4C1	Cytochrome P450 4C1	Worker
LOC105831887	pos	pos	neut	2.15	1.76	0.01743138	Lysine-specific demethylase 6A	Putative uncharacterized protein (Fragment)	Worker

External Database S1.

Complete list of genes summarizing the per-locus results of differential expression analyses, population genomic analyses, and phylostratigraphy analyses. Columns show: annotation from SwissProt and UniProt; results from differential expression analysis by larval stage (L2-L5), adult head and gaster (abdominal) tissue, across all larval samples, and across all samples, with levels NDE = non differentially expressed genes, Reproductive = reproductive-upregulated, and Worker = worker-upregulated; counts of nonsynonymous and synonymous polymorphisms within *M. pharaonis* and fixed differences between *M. pharaonis* and *M. chinense*, and total numbers of nonsynonymous and synonymous sites; results from SnIPRE analysis including BSnIPRE.class, whether genes are categorized by SnIPRE as experiencing positive selection ("pos"), negative selection ("neg"), or neither ("neut"), BSnIPRE.gamma, a population-size calibrated selection coefficient estimate, and BSnIPRE.est, normalized BSnIPRE.gamma; "NI.class" refers to selection categories, as calculated using a combination of the neutrality index and the p-value from the McDonald-Kreitman test: Genes with negative values of -log10(Neutrality Index) and p-values less than 0.05 are defined as under purifying selection, while such genes with positive -log10(Neutrality Index) values are assigned to the positive selection category. "NI.class B-F correction" uses the same method but the p-value cutoff from the McDonald-Kreitman is adjusted for multiple comparisons using the Bonferroni procedure; Finally, the assigned raw ("Raw PS") and condensed phylostrata ("PS1" and "PS2"; Table S4) from the phylostratigraphy analyses are shown.

External Database S2.

Complete GO enrichment analysis results for workers and reproductives for each differential expression test, as calculated using the R package GOstats, sorted by p-value. L2 not included due to paucity of differentially expressed genes.

External Database S3.

Complete GO enrichment analysis results for each phylostrata category for each differential expression test, as calculated using the R package GOstats, sorted by p-value. L2 not included due to paucity of differentially expressed genes. Missing phylostrata categories returned no significant GO terms.

External Database S4.

Raw counts per locus from RNA sequencing showing level of expression across all samples included in the study (Table S1).

External Database S5.

Raw FPKM per locus from RNA sequencing showing level of expression across all samples included in the study (Table S1).